CCDs- Ideal and not-so-ideal, in the LSST context

Christopher Stubbs
Harvard University
stubbs@physics.harvard.edu

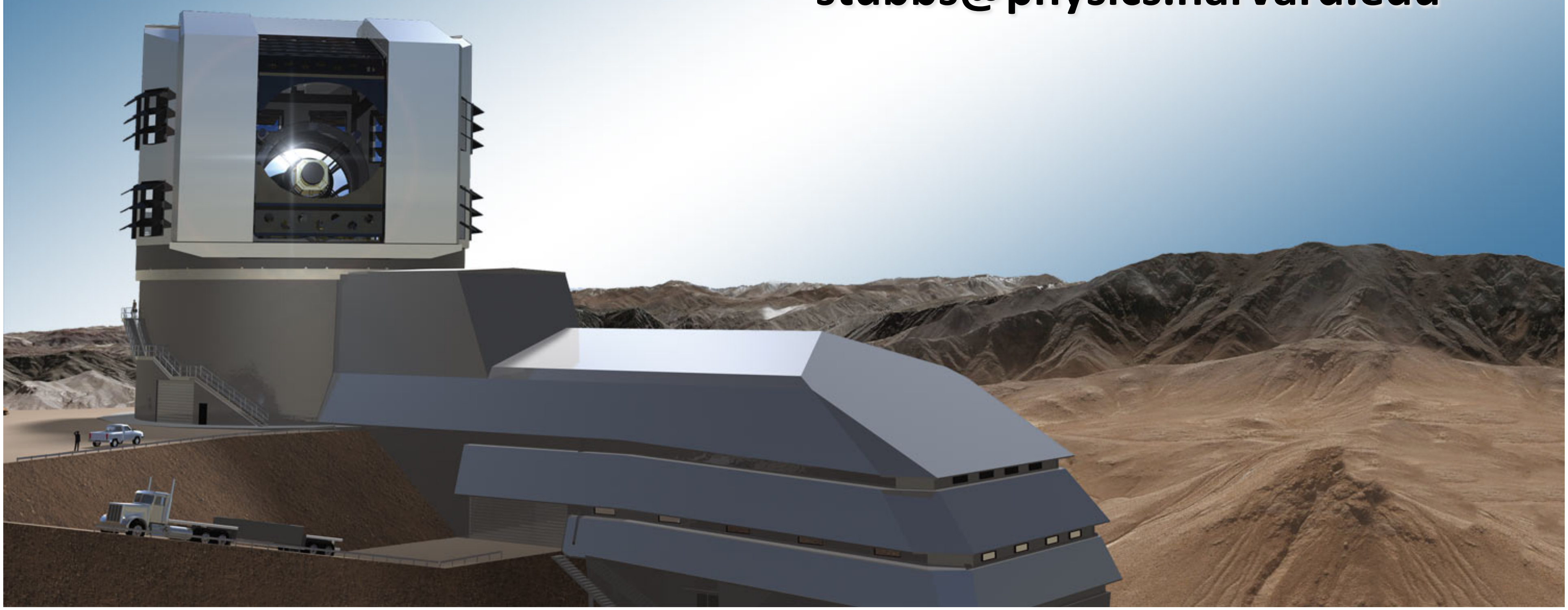

Outline

- Motivations for higher precision measurements
- The LSST project and its objectives
- Quick introduction to how CCDs work
- LSST sensor design choices
- Lateral Electric Fields and CCD Pathologies
    - Edge Rolloff
    - Intensity-dependent PSF's
    - Tree rings
- Some resources and references

LSST's need for high precision measurements

• Measuring dark energy properties using type Ia supernovae is presently limited by photometric calibration issues, at the 1% level.

• LSST (from ground), Euclid, and WFIRST (from space) intend to measure correlations between subtle shape distortions of galaxies across widely separated fields on the sky. This analysis requires disentangling atmospheric distortion and sensor artifacts from actual underlying galaxy shapes.

• Photo-z's require reliable determinations of galaxy colors.

• Frame subtraction and frame co-addition both require a full understanding of the point spread function (PSF*) of the system

*The PSF is the observed distribution of photoelectrons in the CCD array due to an unresolved (point) source in the sky. This is primarily governed by atmospheric "seeing", by low-angle scattering, and by sensor effects.

Some Editorial Comments

• The astronomical instrumentation community has misinterpreted flatfields for decades, and have in many (most?) cases been *introducing* errors that limit measurement precision. Naïve flat-fielding is a bad thing.

• Many (all?) of the effects we see in deep depletion CCDs are exaggerated versions of phenomena that do afflict traditional CCDs.

• The "precision frontier" in astronomical measurements will yield substantial scientific gains. We are nowhere near the Poisson limit for precise flux measurements when N_e>1000, for example.

• The optical/IR astronomical instrumentation community seldom invests the time and effort needed to truly understand the nuances of their instruments. Tendency for teams to produce a system, put it on the sky, and move on to writing the proposal for the next instrument. Science suffers as a result.

The Large Synoptic Survey Telescope Wallet Card

- Three Mirror Anastigmat (TMA) optical design.
  - 8.4 meter primary, 6.5 meter effective aperture
  - 3.4 meter diameter secondary
  - 5 m tertiary is being fabricated in same substrate as primary mirror
  - three-element refractive corrector
  - f/1.2 beam delivered to camera
  - 9.6 square degree field (on science imaging pixels)
  - optics deliver < 0.2 arcsec FWHM spot diagram,
  - 6 filters: ugrizy: 320 nm to 1050 nm (UV atmospheric cutoff to Si bandgap)

- 3.0 Gpixel camera
  - 10 micron pixels, 0.2 arcsec/pixel
  - Deep depletion (100 μm), high-resistivity CCDs for NIR response
  - Dual 15 second exposures (to avoid trailing of solar system objects)
    - 2 second readout (trade between noise and imaging efficiency)
    - 550 kpix/sec through 16 amps/CCD x 189 CCDs = 3024 channels
    - 12 GBytes per image (as floating point numbers), 20 TBytes/night.

- Real-time frame subtraction for time domain alerts, ~850 visits for each patch of sky, allows co-adds to r ~ 27 (AB), over 18,000 square degrees.

LSST Camera Sub-System

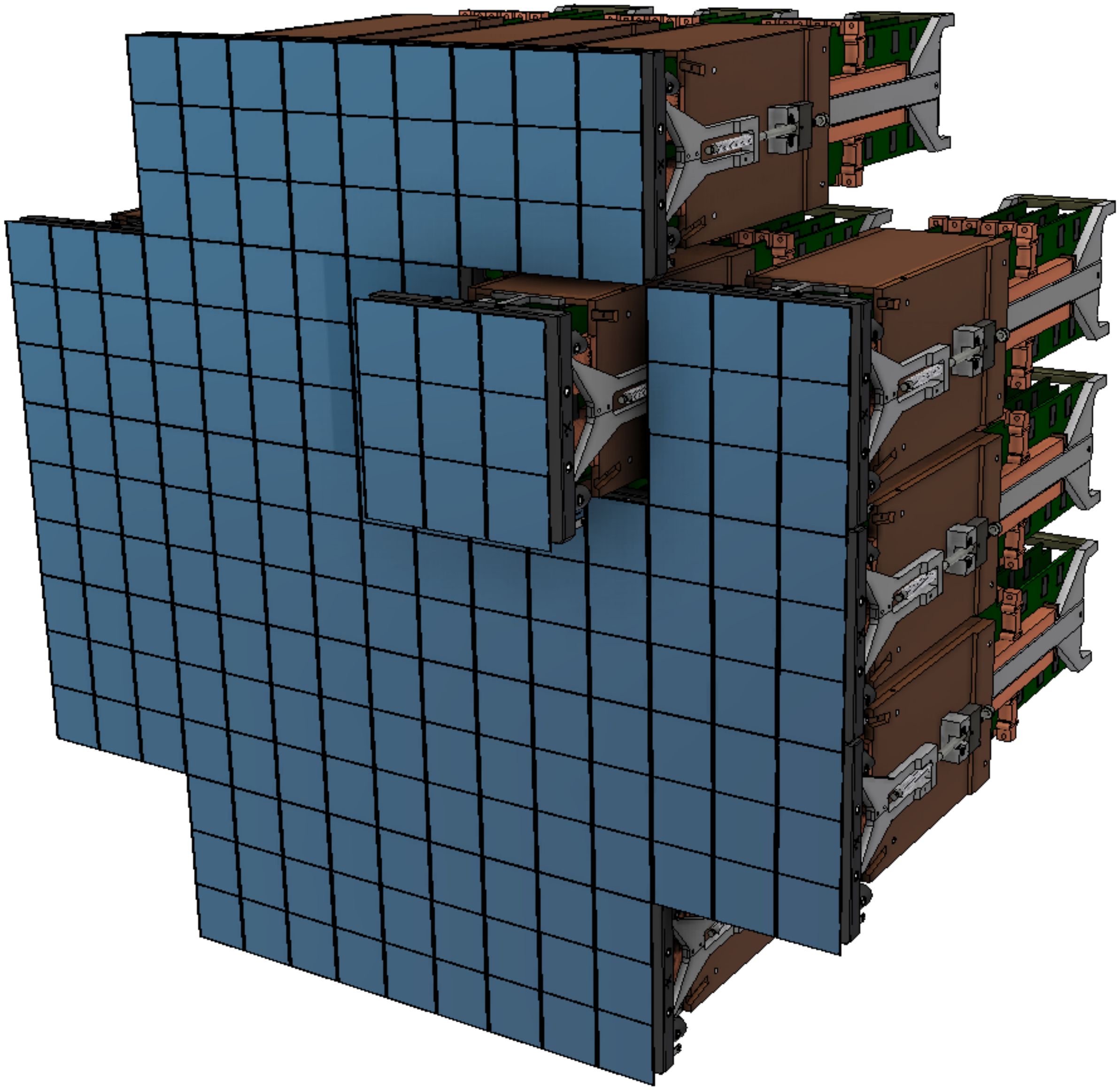

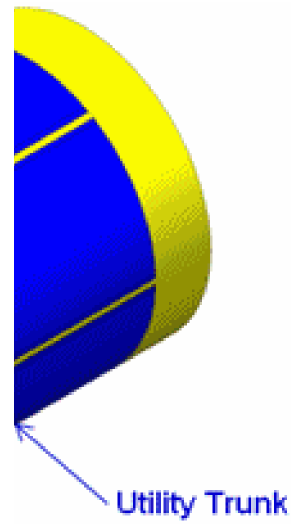

a weight ~ 3 tons

21 science rafts, 189 4K x 4K CCDs

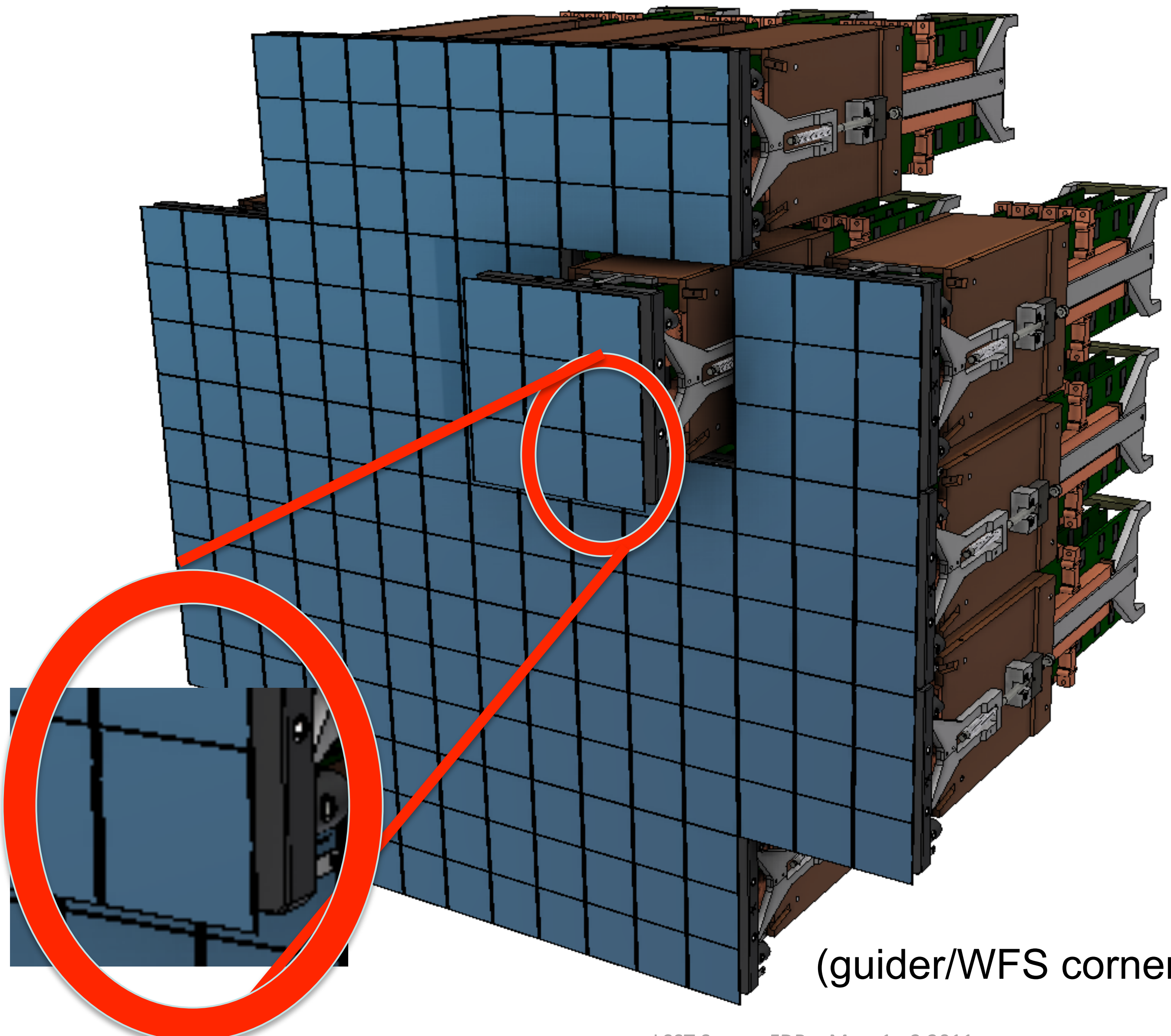

21 "rafts"

9 CCDs per raft

3 CCDs per board

Focal plane: −100C

Boards: −40C

(guider/WFS corner rafts not shown)

Two candidate vendors for LSST CCDs: ITL and e2v.

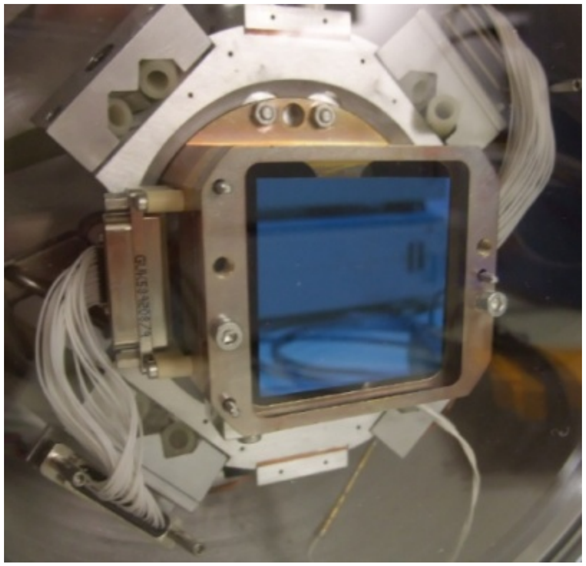

E2V

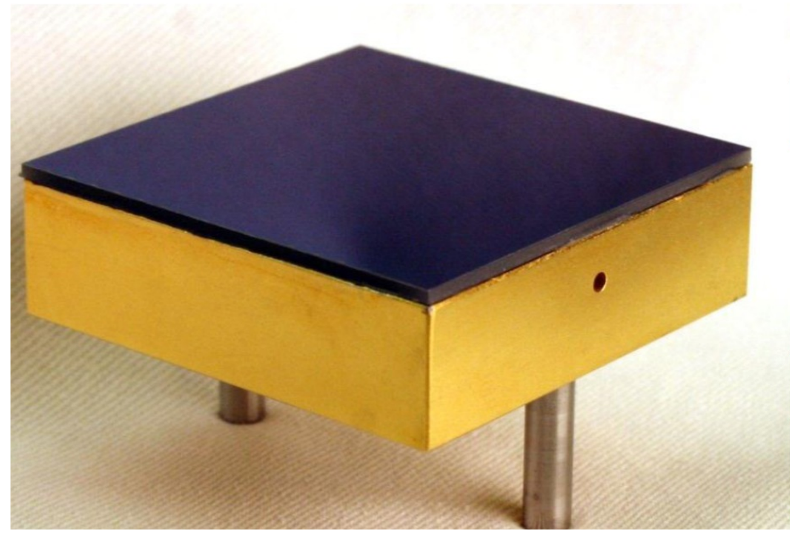

ITL

The LSST CCDs differ from those in current use- thicker and faster readout.

How CCDs work, I

- Silicon is a semiconductor.
- Incident photons with energy greater than the bandgap can promote charge carriers into the conduction band.
- These photoelectrons are produced in the device, and a vertical electric field drives them down into the pixel structure where they are stored until readout.
- A pixel is defined by channel stops in x direction and biased gates in y

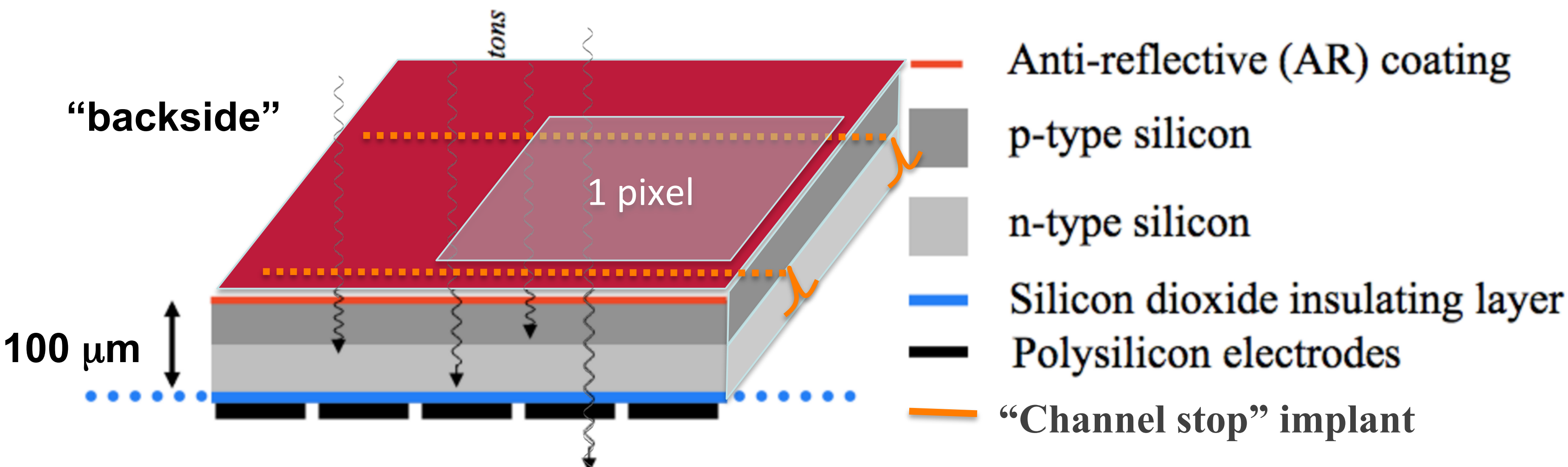

http://www.vikdhillon.staff.shef.ac.uk/teaching/phy217/detectors/phy217_det_performance.html

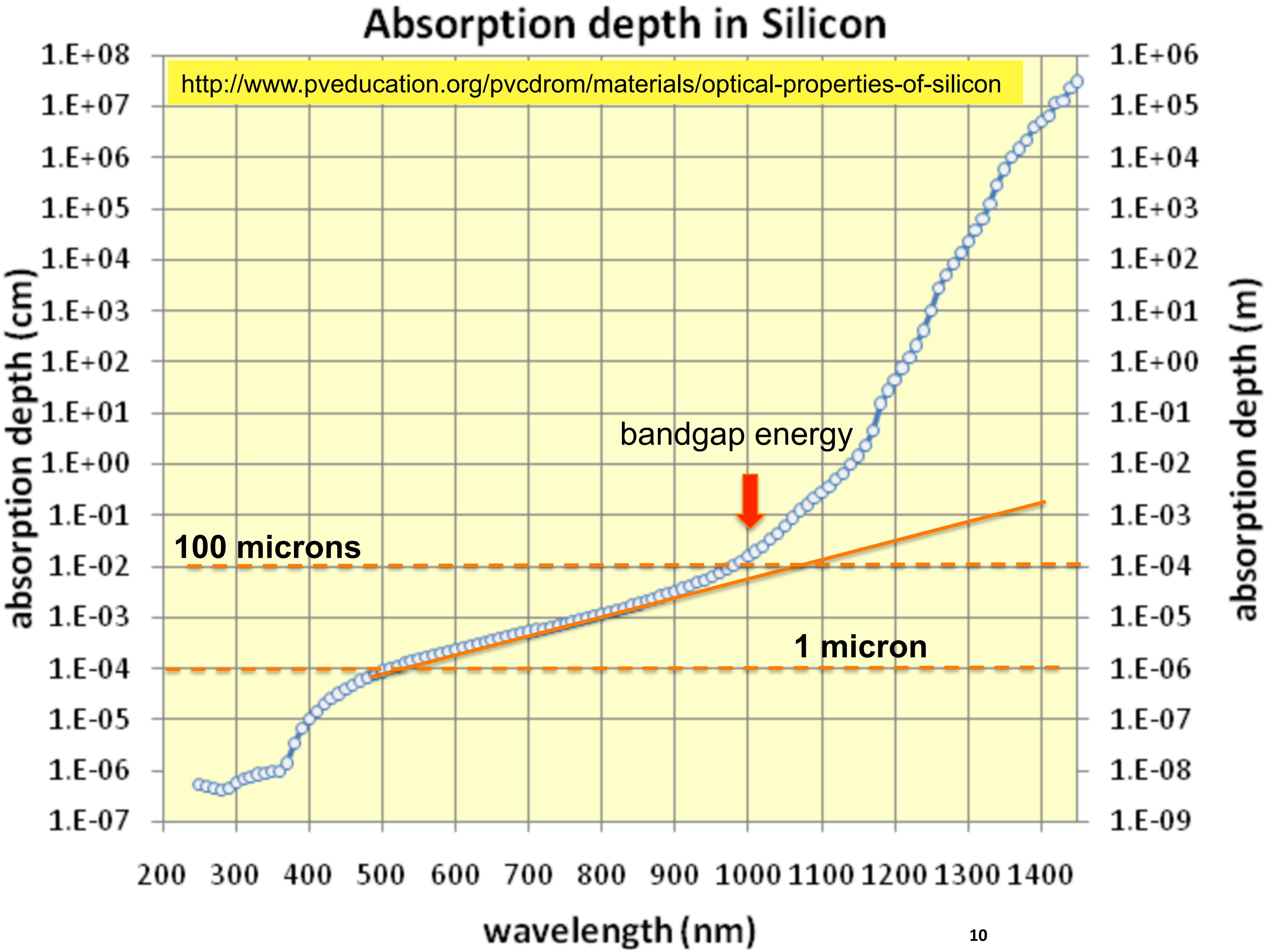

Absorption depth in Silicon
http://www.pveducation.org/pvcdrom/materials/optical-properties-of-silicon
bandgap energy
100 microns
1 micron
absorption depth (cm)
absorption depth (m)
wavelength (nm)
1.E+08
1.E+07
1.E+06
1.E+05
1.E+04
1.E+03
1.E+02
1.E+01
1.E+00
1.E-01
1.E-02
1.E-03
1.E-04
1.E-05
1.E-06
1.E-07
1.E-08
1.E-09
200 300 400 500 600 700 800 900 1000 1100 1200 1300 1400

Most photons convert near the backside surface

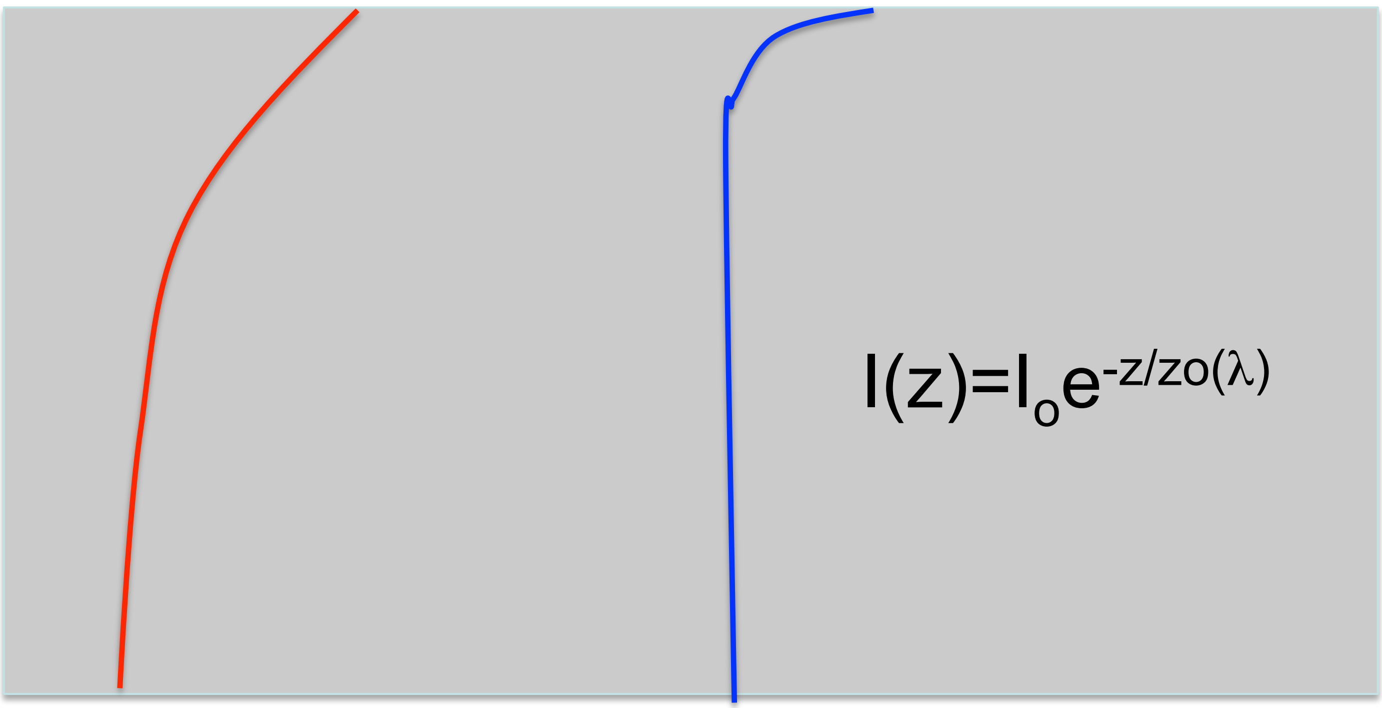

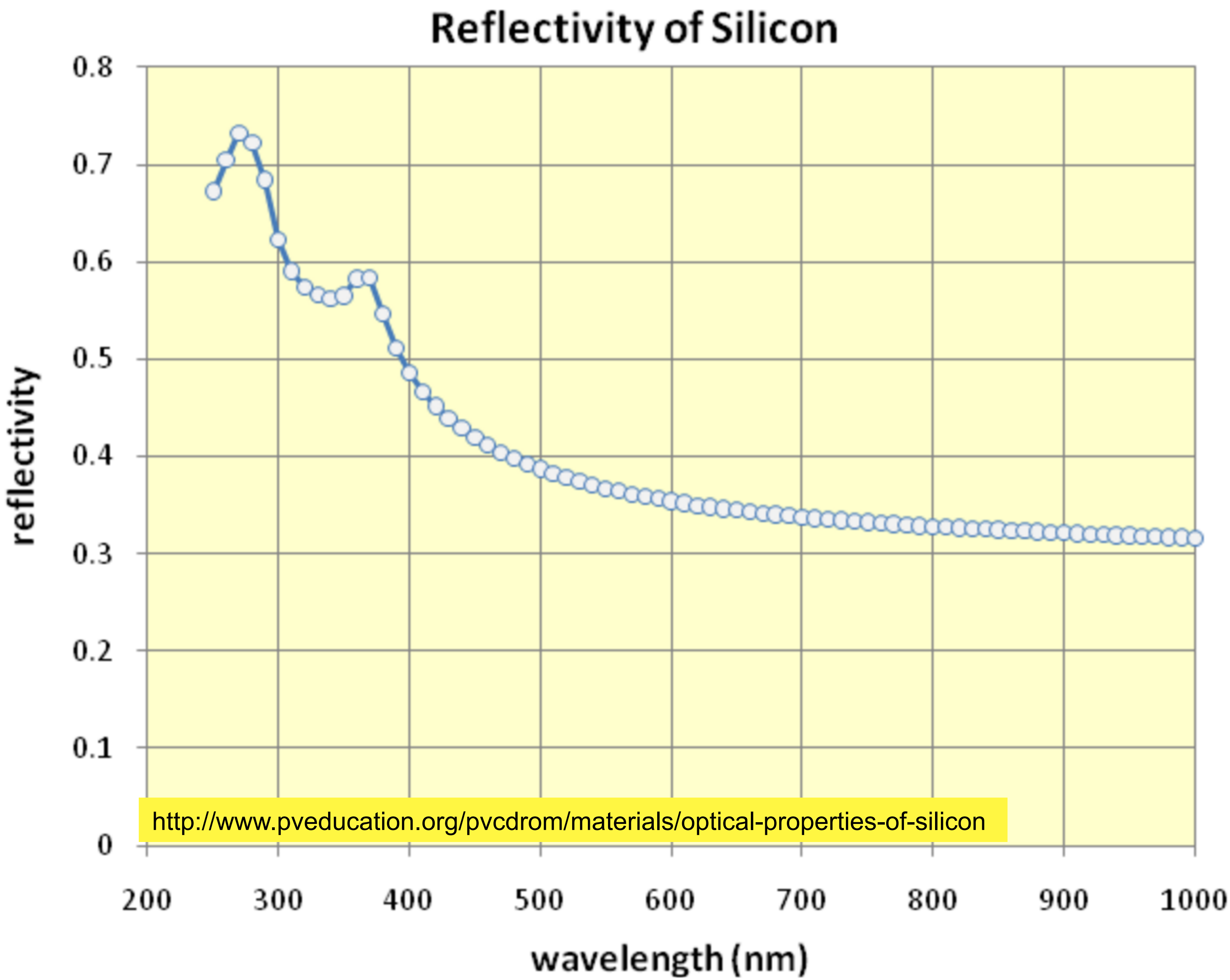
Reflectivity of Silicon
reflectivity
0.8
0.7
0.6
0.5
0.4
0.3
0.2
0.1
0
200
300
400
500
600
700
800
900
1000
wavelength (nm)
http://www.pveducation.org/pvcdrom/materials/optical-properties-of-silicon

How CCDs work, II

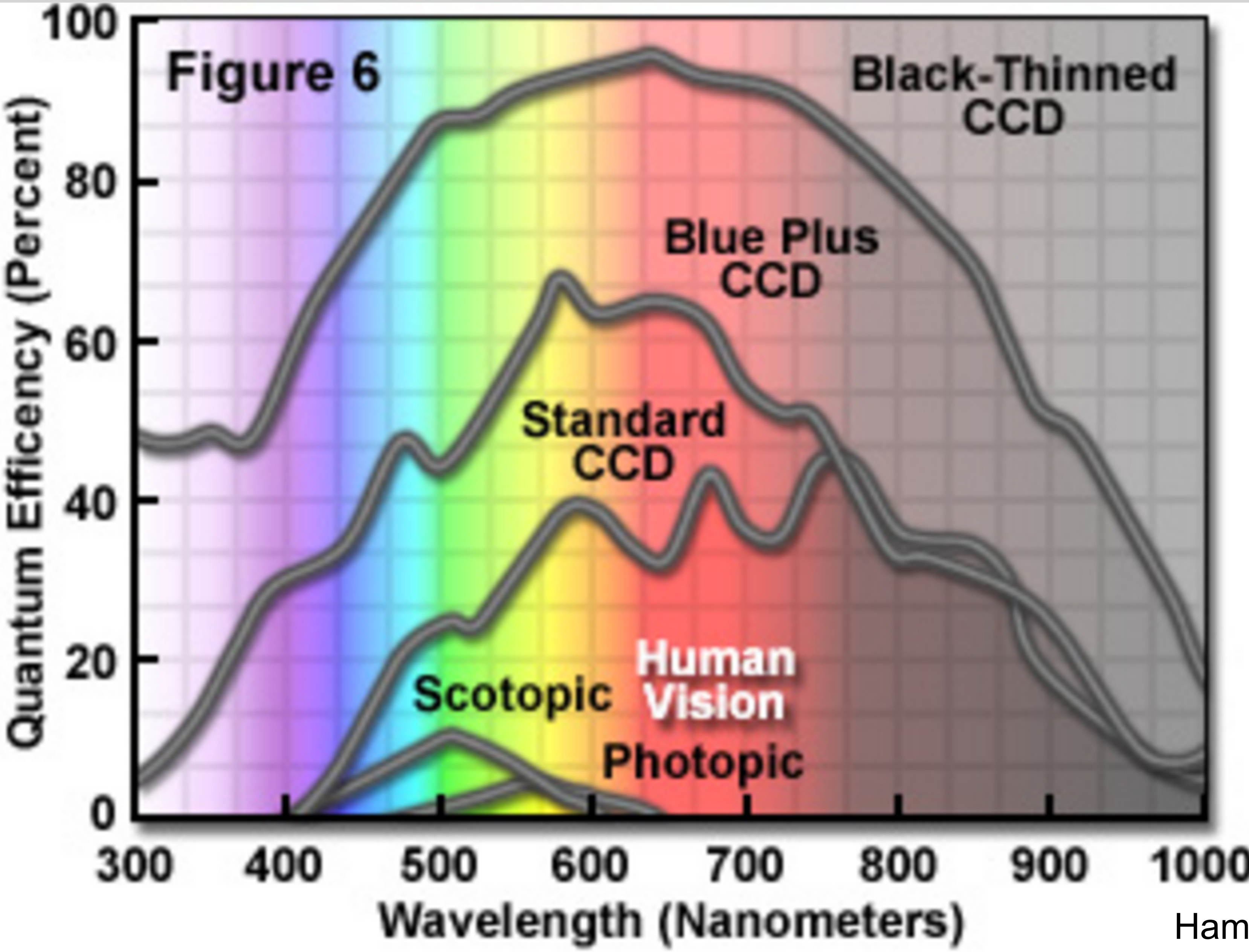

Hamamatsu

Parallel and serial charge transfer for CCD readout

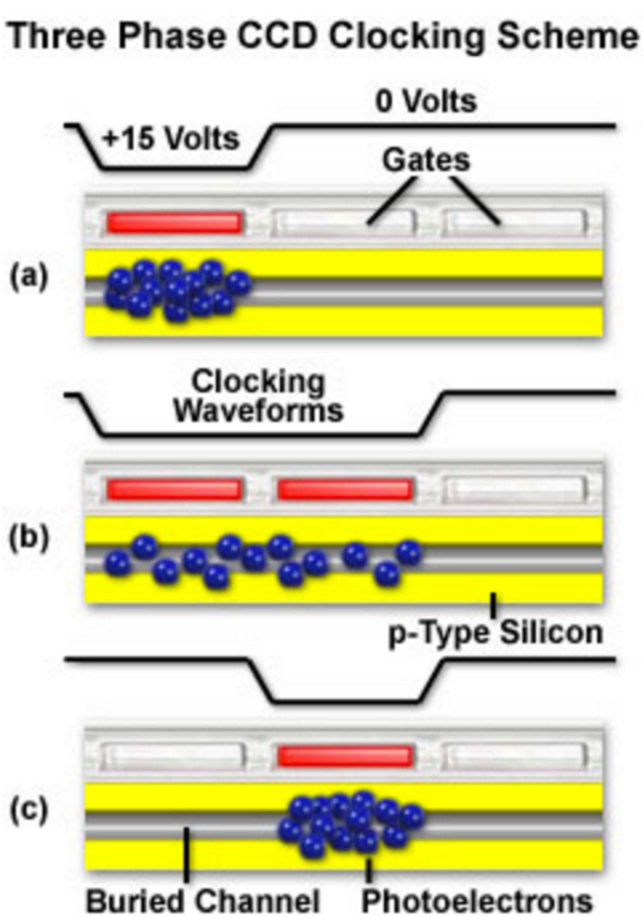

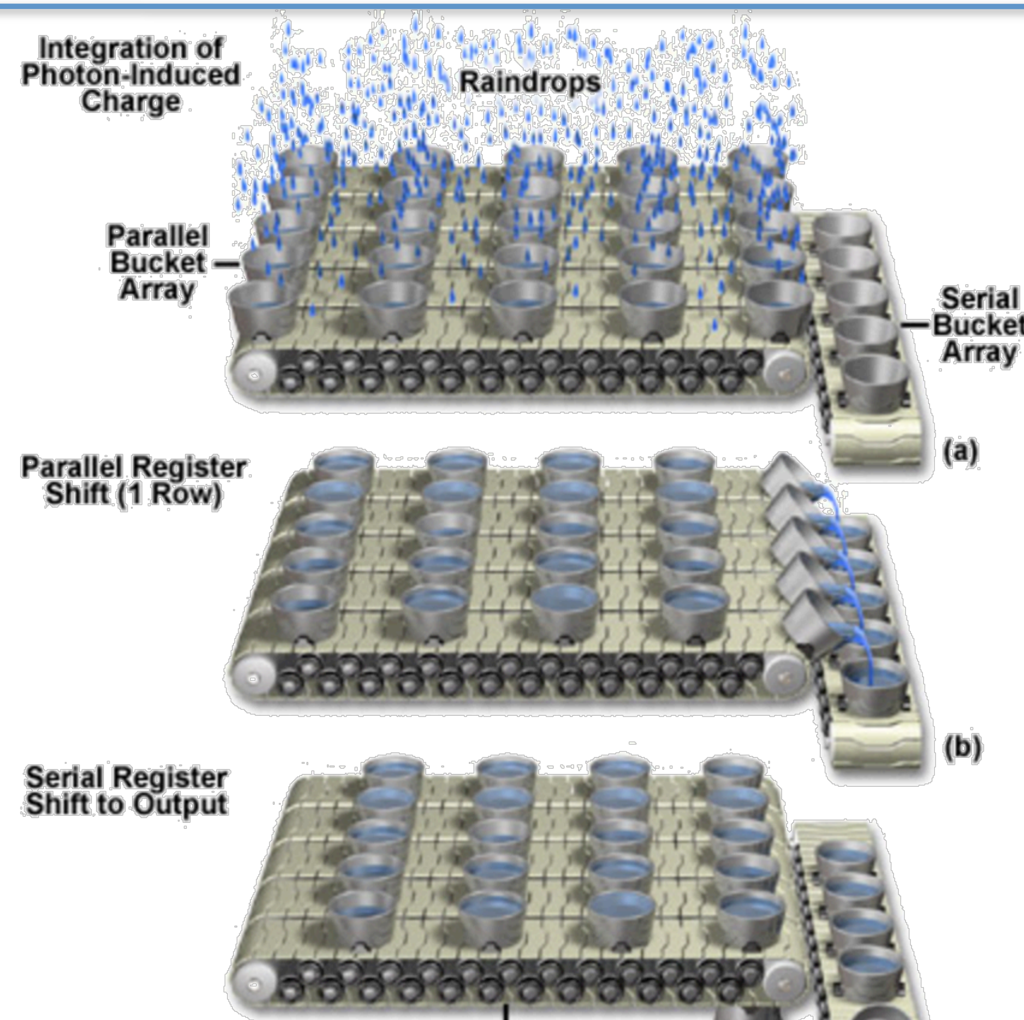

Figure 5

Bucket Brigade CCD Analogy

https://www.microscopyu.com/articles/digitalimaging/ccdintro.html

LSST sensors are thick, highly-multiplexed, and expensive

- 100μm-thick, high resistivity silicon CCDs, fully-depleted with transparent conductive window and AR coating
  - *for broadband QE and small PSF*
- 4K x 4K format
  - *4 die sites/6" wafer*
- 16-fold parallel output
  - *for low noise readout at 2s frame read time*
- 10μm pixels
  - *for optimum sampling of LSST PSF, at 0.2 arcsec/pixel*
- Buttable, thermally-matched packaging
  - *>92% fill factor*
- Flatness and coplanarity to bring image surface within ±0.009mm from baseplate
  - *for use in fast f/1.2 beam*
- Mechanical mounting and alignment features and electrical interface specified
  - *Interchangeability between vendors*
- Sensor contracts for initial production awarded to two vendors

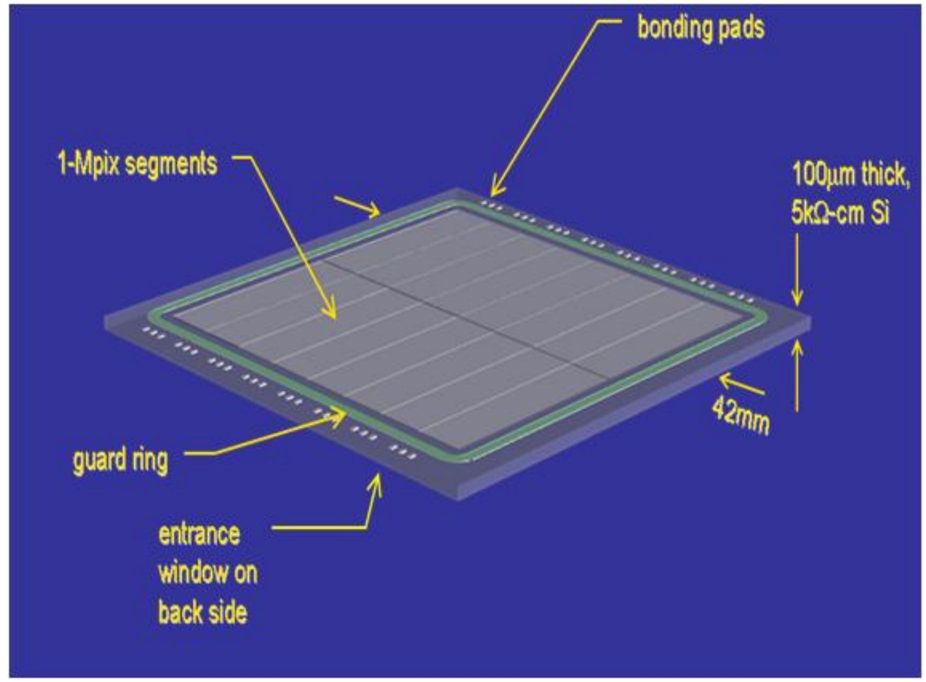

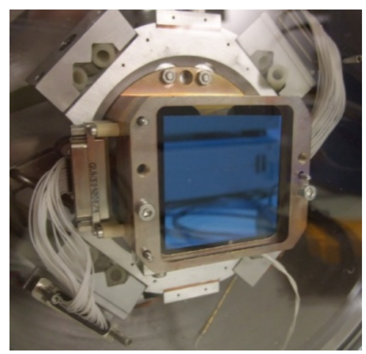

E2V

ITL

“The only uniform CCD is a dead CCD” – Craig McKay

Performance Aspect	Ideal CCD	Real CCD
Noise with no charge (read noise)	zero	3-10 electrons rms
Charge transfer eff.	1.000000	0.99999
Quantum efficiency	1.0, no structure	0.3 to 0.95, structured
R^2 <->R^2 mapping of image into pixels	devoid of structure	distortions
Point spread function (PSF)	intensity-independent	brighter-fatter effect!
Crosstalk between analog channels	zero	10^{-3}
Statistics	Pure Poisson-limited	Departures from Poisson
Dynamic range- max. charge per pixel	infinite	~100,000 e
Defects- hot pixels, dead pixels…	none	some
Temperature and temporal dependence of gain, CTE, defects, etc	none	some

One aspect of astronomical image processing is to correct for all these effects

Some characteristics of deep depletion CCDs that merit our attention – for PanSTARRS, DES and LSST.

• Lateral electric fields at edges and within the array produce charge transport effects that can masquerade as quantum efficiency variations.

• Image persistence produces systematic errors in subsequent images.

• "Tree rings" of impurities in Si are evident in flatfields, and this using these flats generates astrometric, photometric and shape distortions.

• Trapped holes can produce time-variable perturbations in the array, that can't be overcome with static additive (bias) or multiplicative (flatfielding) corrections.

• Some deep depletion sensors are damaged by exposure to high light levels.

• Space charge effects repel incident photoelectrons from pixels with substantial accumulated charge. This introduces correlations that violate Poisson statistics, giving weird photon transfer curves and intensity-dependent PSF's. Most weak lensing and photometric and astrometric analysis codes assume identical PSF for faint and bright objects.

LSST detector, side view: towers of Silicon!

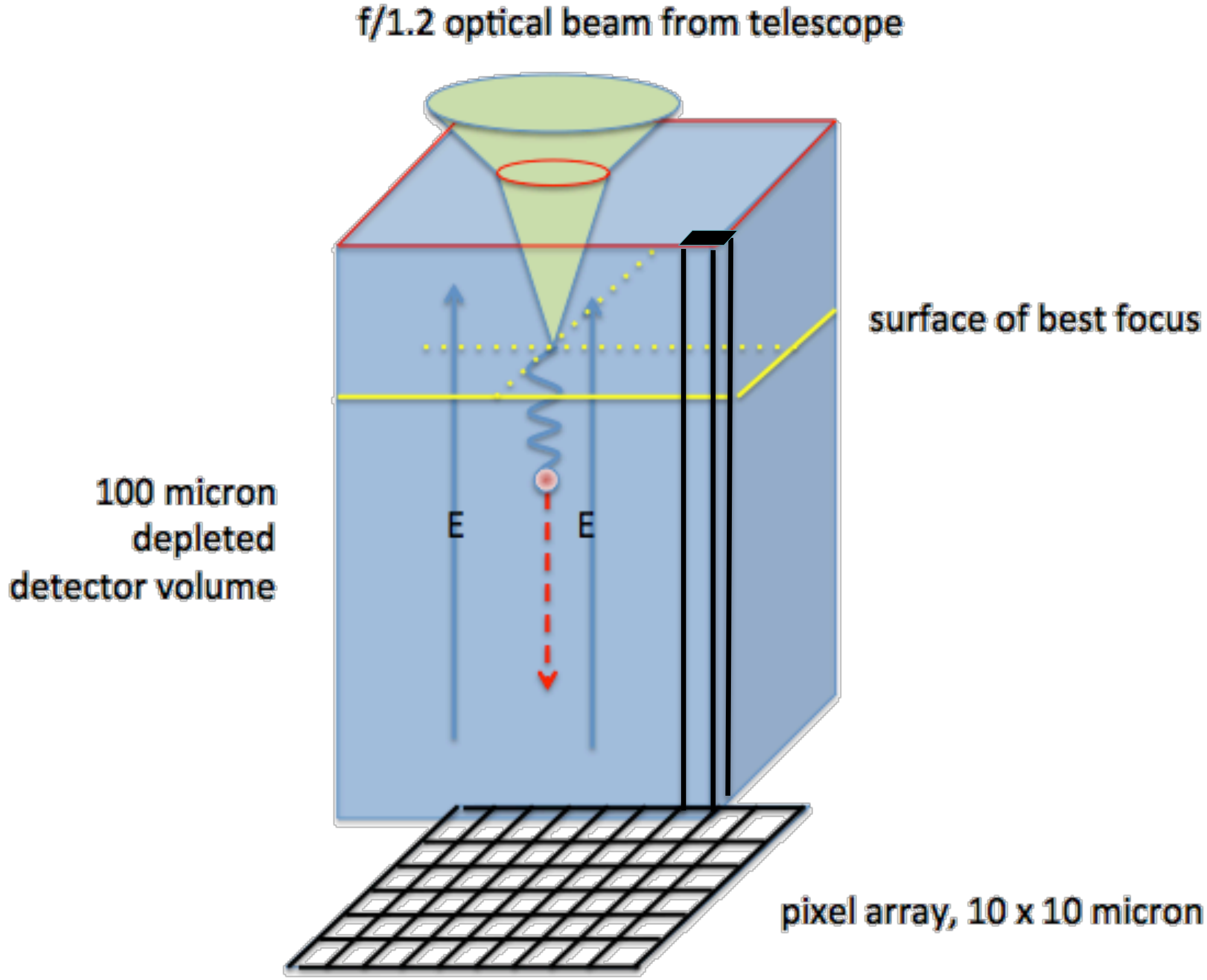

Flux roll-off in flats, at edges of sensor

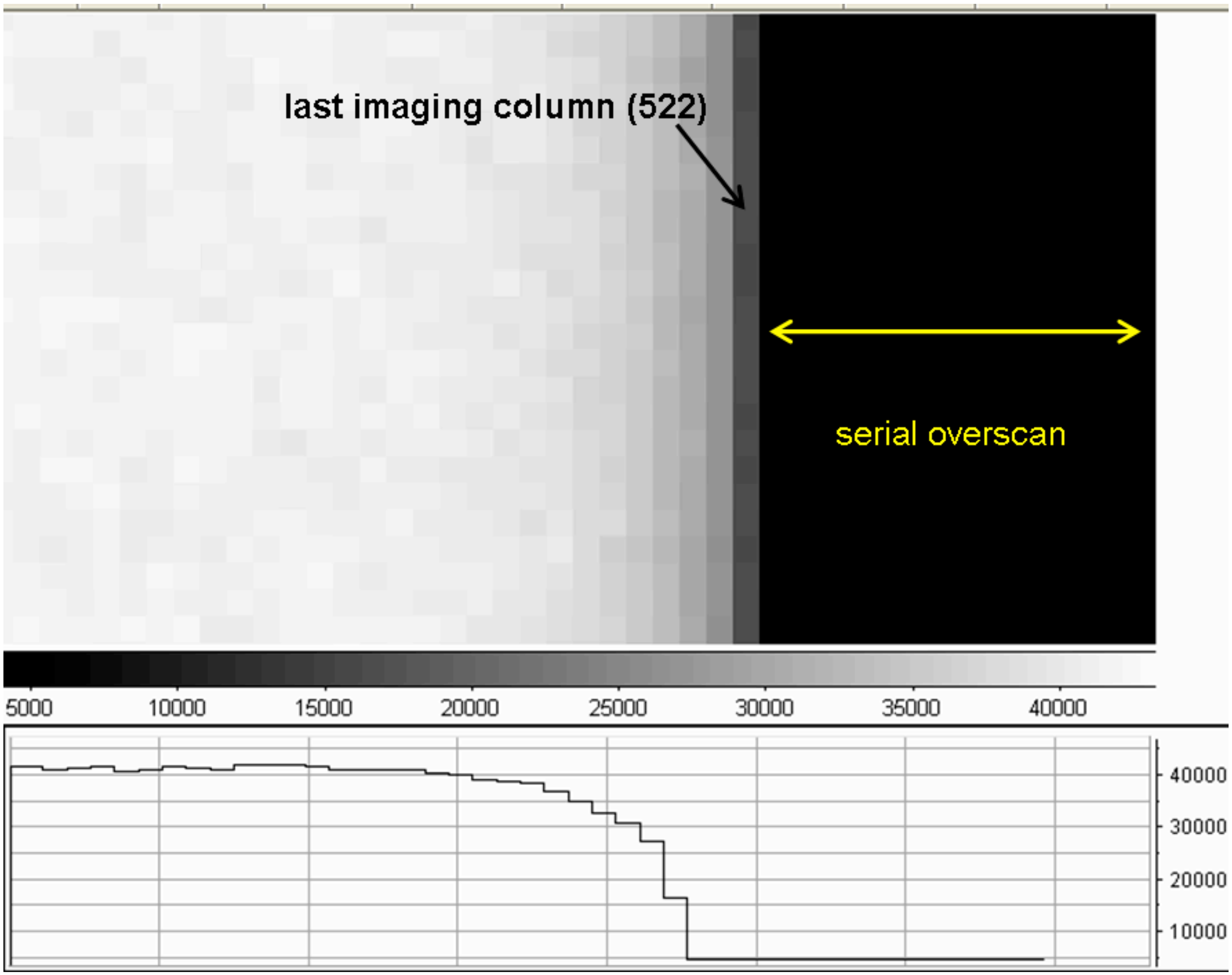

Scanned Spots- measure (x,y,Φ) & PSF

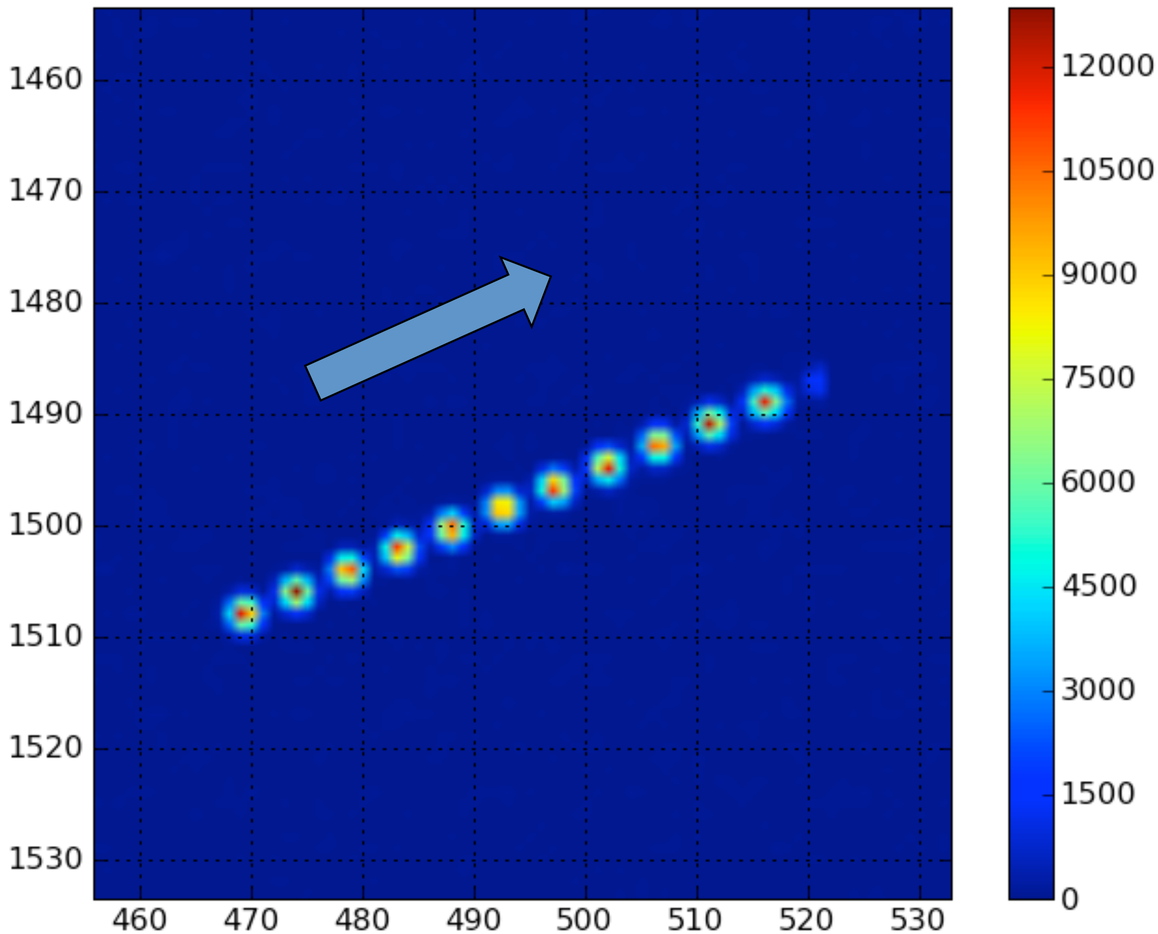

Photometric Analysis of Spot Data

Spot flux does not trace flatfield flux

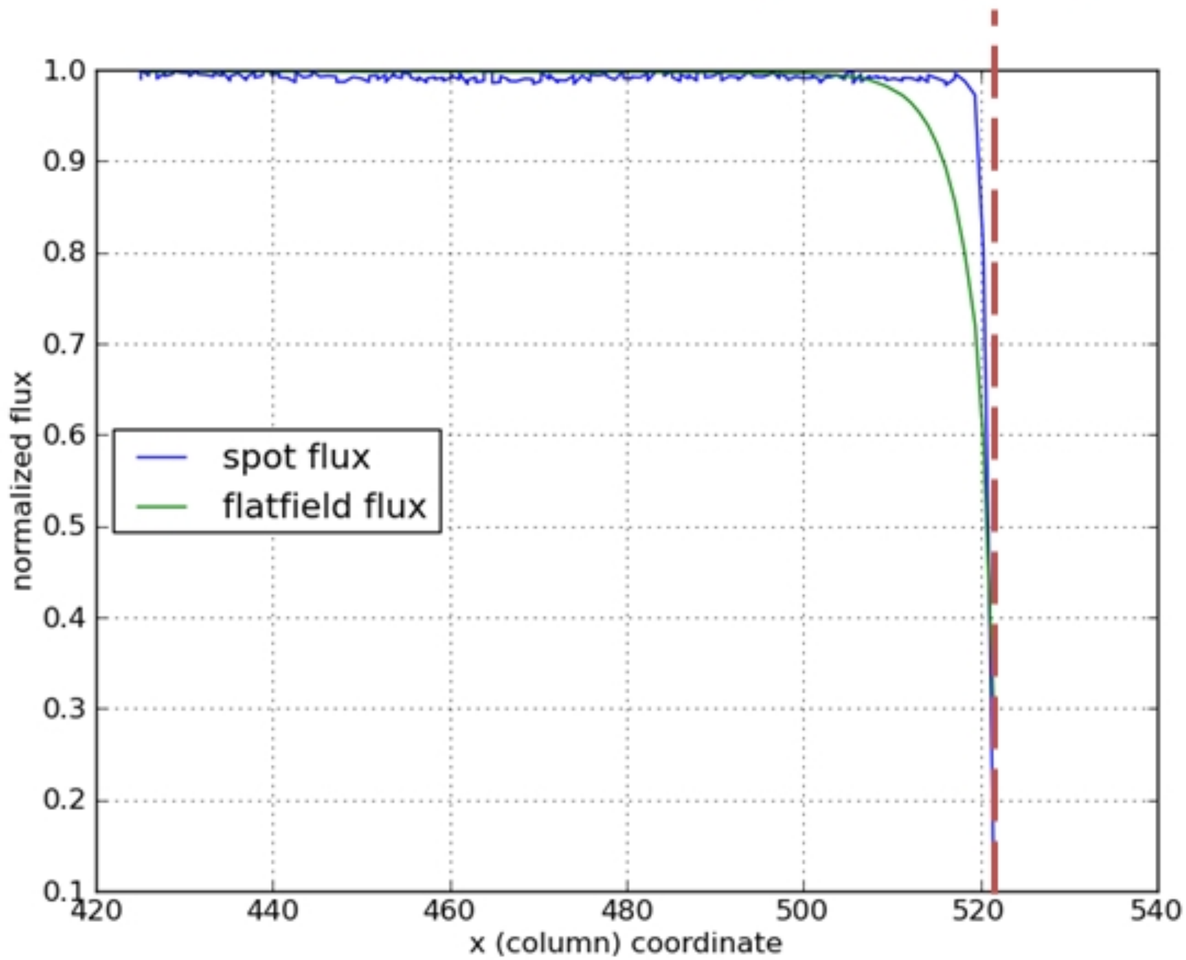

Guard ring electrode attracts electrons from both sides

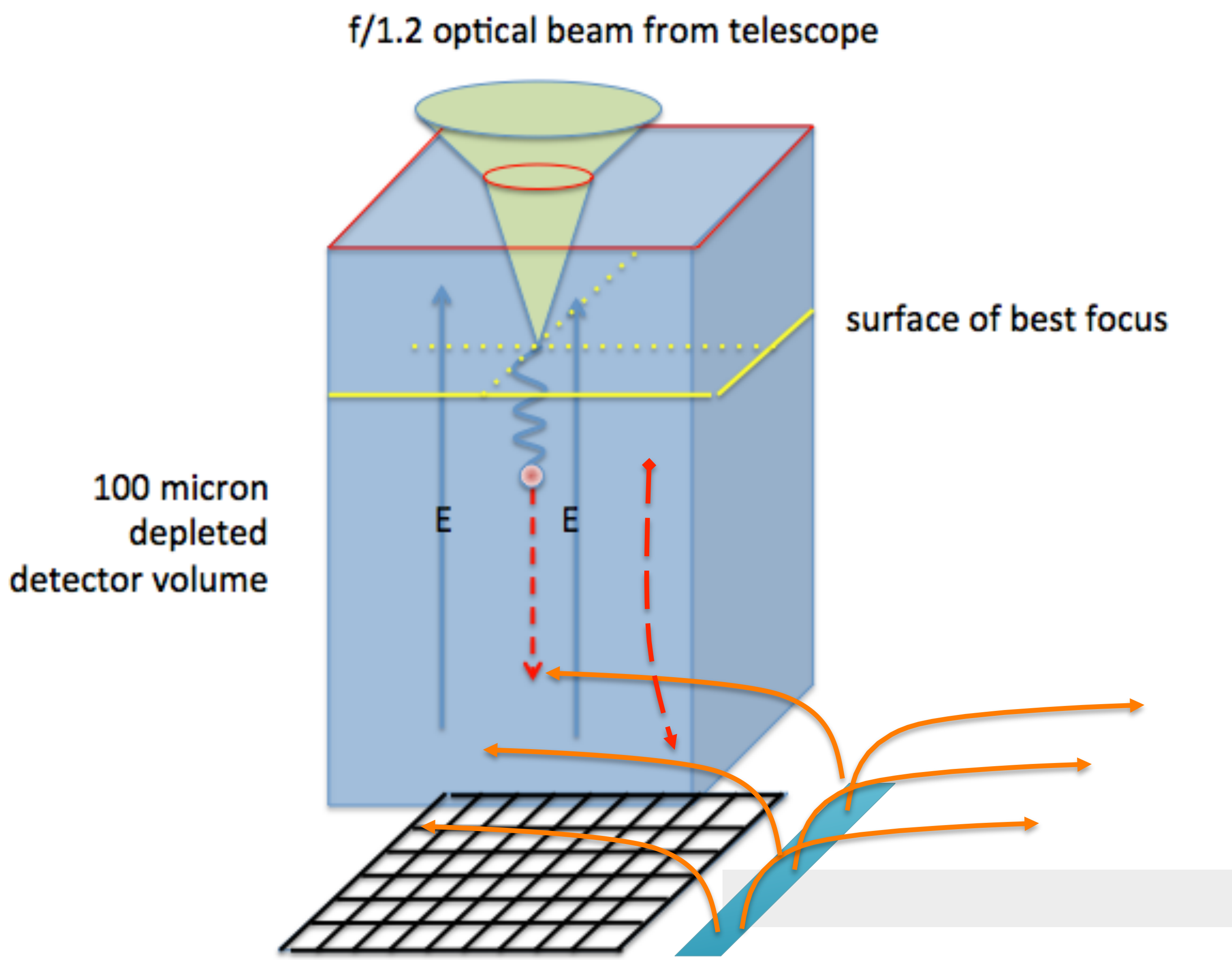

Interpretation of Observed Phenomenology- surface brightness from flats is attenuated, but point source flux is constant, up to Si edge.

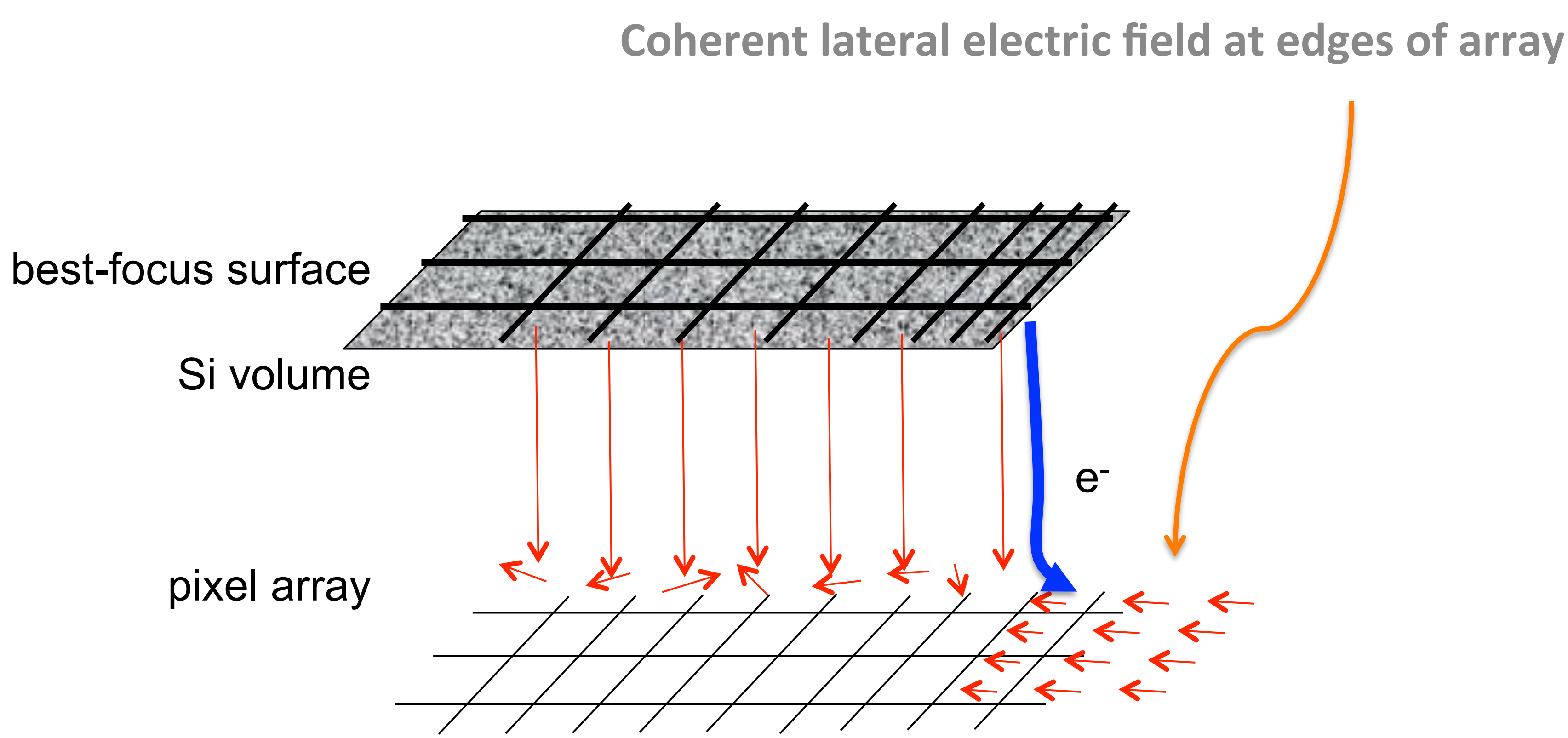

Simulation Algorithm for Edge Rolloff

1. Generate unwarped image
2. Divide each LSST pixel into micropixels
3. Apply exponential warp to micropixel coordinates
4. Populate integer micropixels with scaled data
5. Crop, bin back from micropixels to LSST pixels

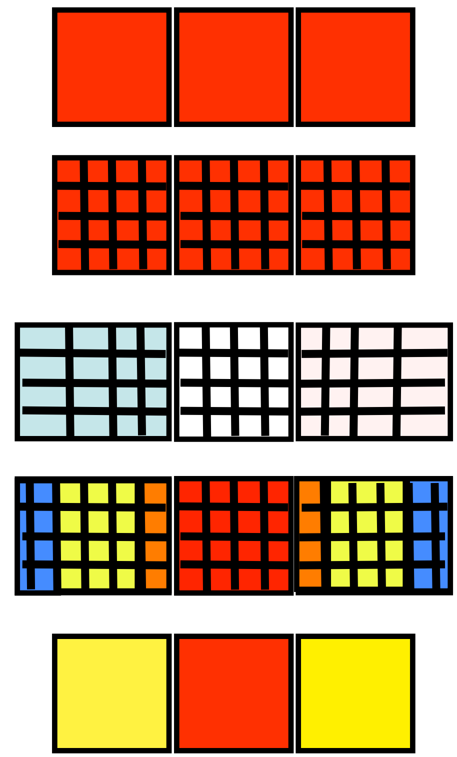

Sample Simulated Images: Flat Field

Original

Warped

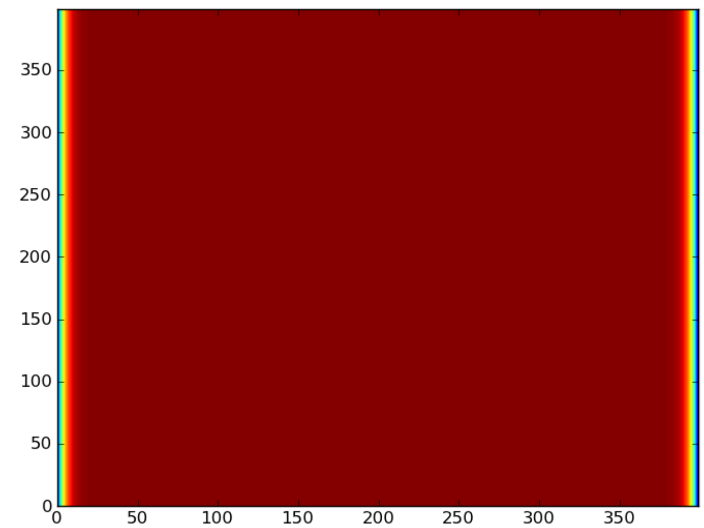

Does this simulation match the data? Yes.

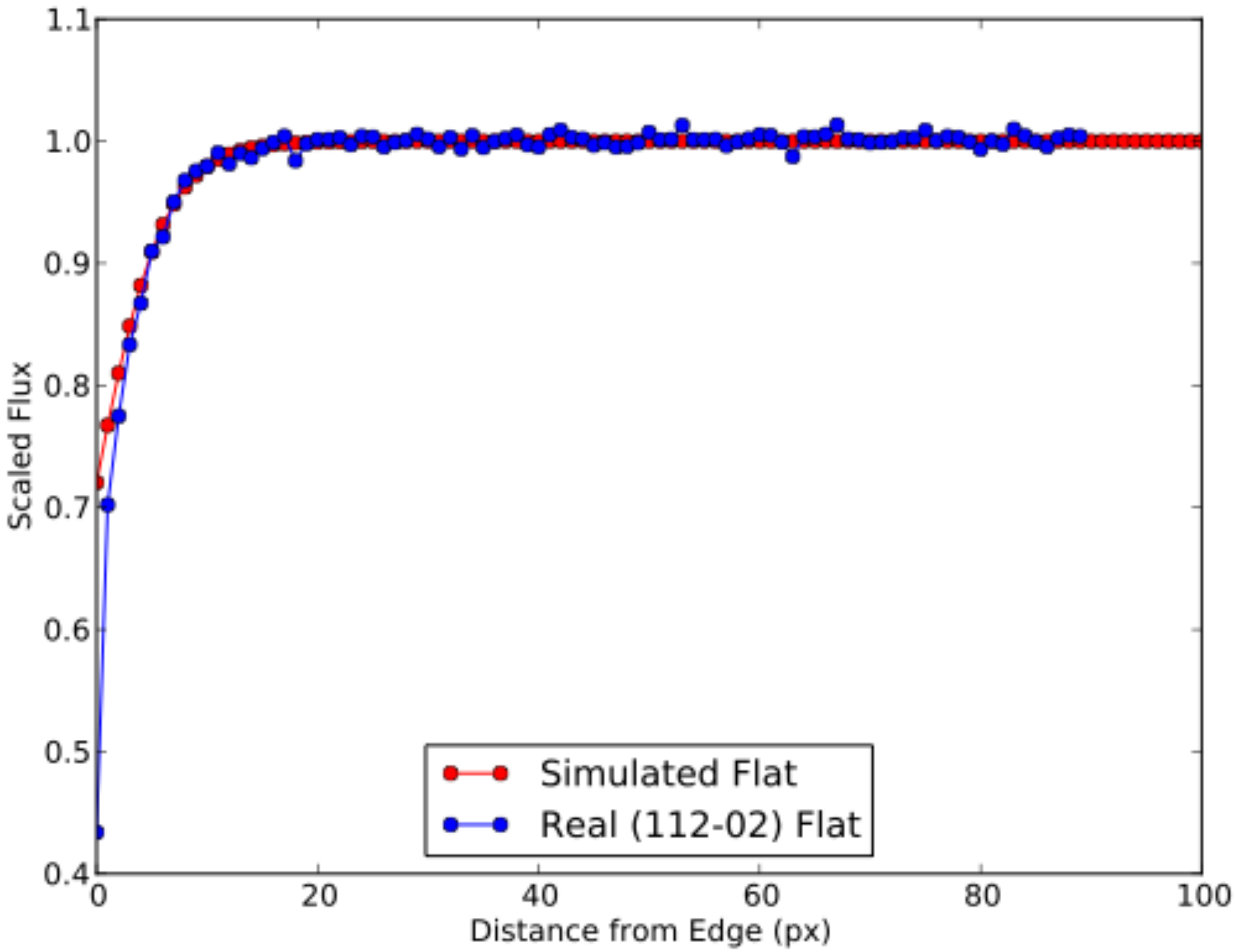

Real and Simulated Rolloff Profiles

Sample Simulated Images: “Stars”

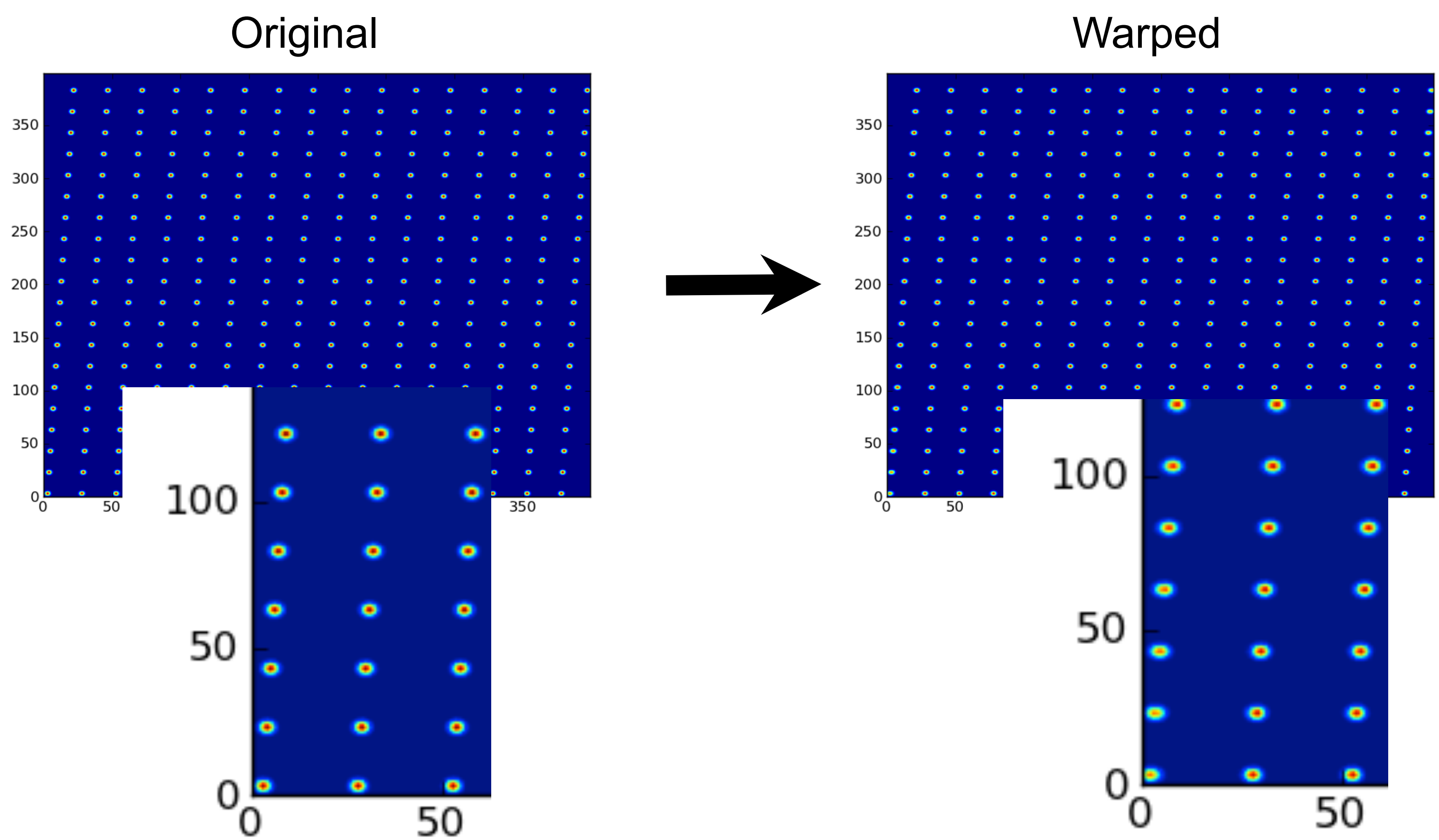

Sample Simulated Images: Exaggerated Lateral Field

Original

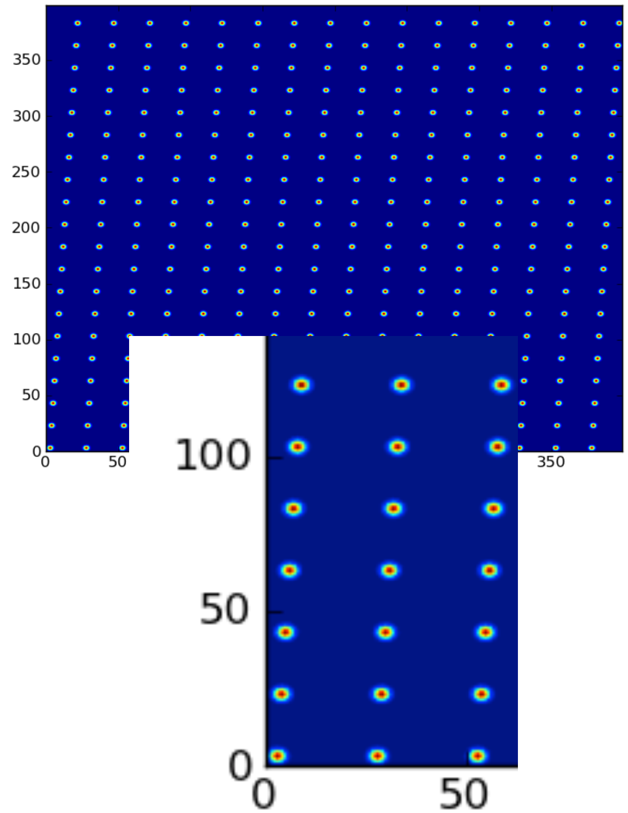

Exaggerated

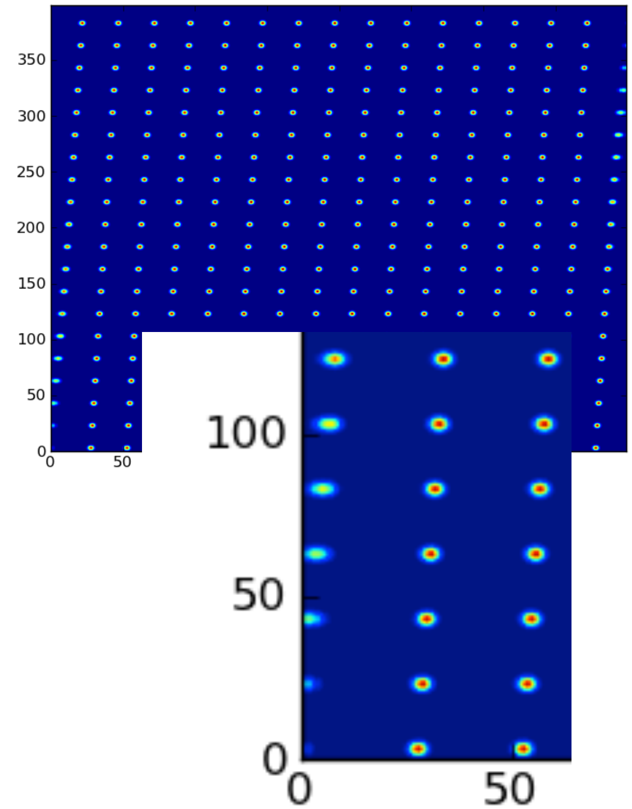

Analysis

Ran Source Extractor on original and warped data

Output aperture mag, PSF mag, FWHM, ellipticity, centroids

We want to know:

- How does warping affect the MAGNITUDE of the star?
- How does warping affect the SHAPE of the star?
- How does warping affect the POSITION of the star?
- What happens if we try to flat-field by a warped flat?

Photometric, Astrometric, and Shape Errors introduced by edge distortion

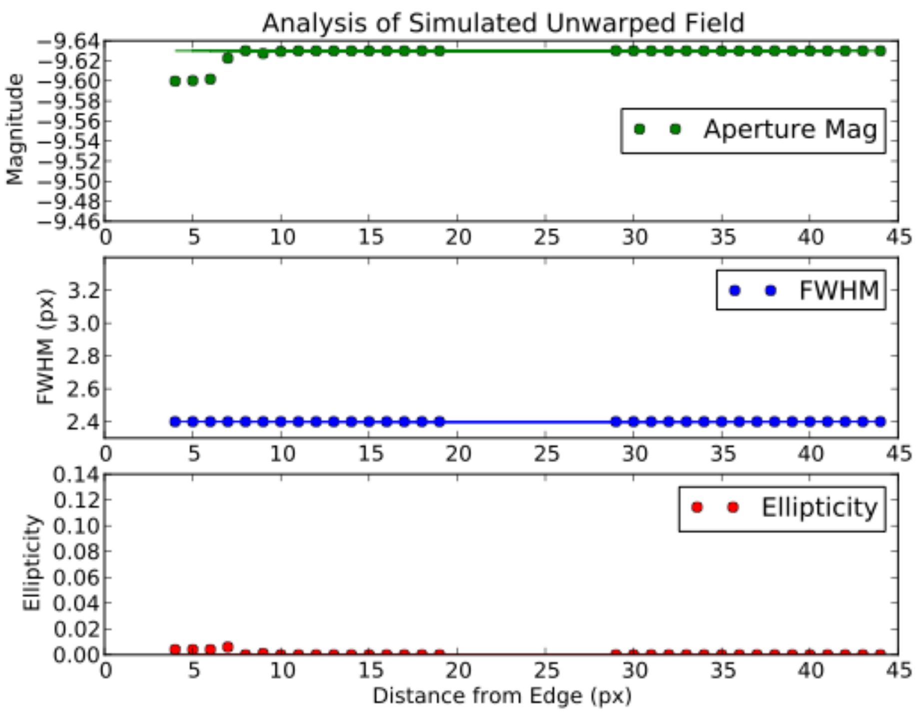

Unwarped Grid of “Stars”

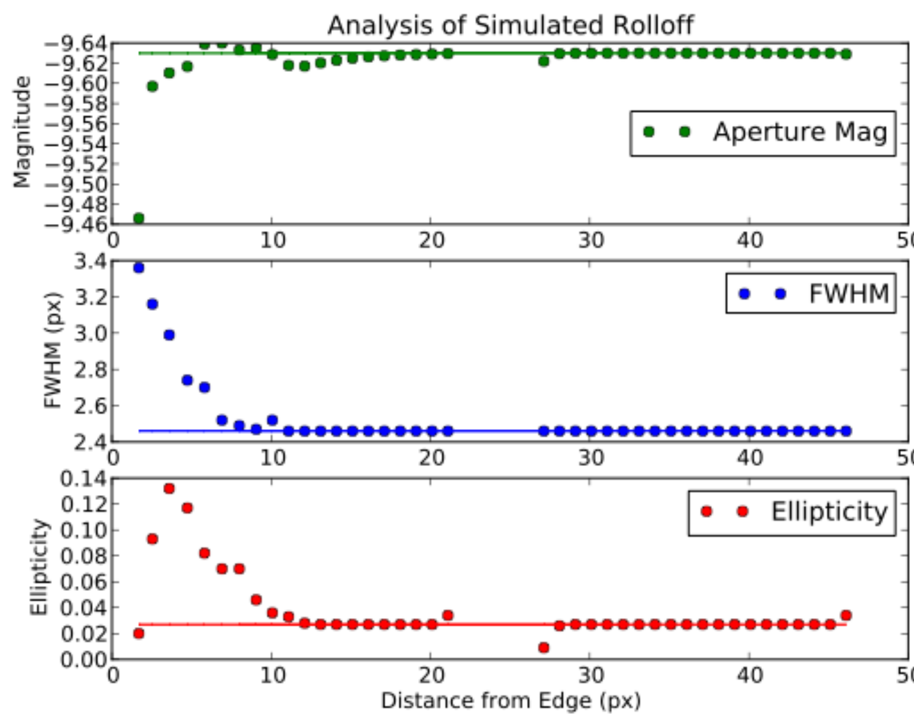

Warped Grid of “Stars”

<u>Substantial</u> Flux Errors Introduced by Inappropriate Flat-Fielding

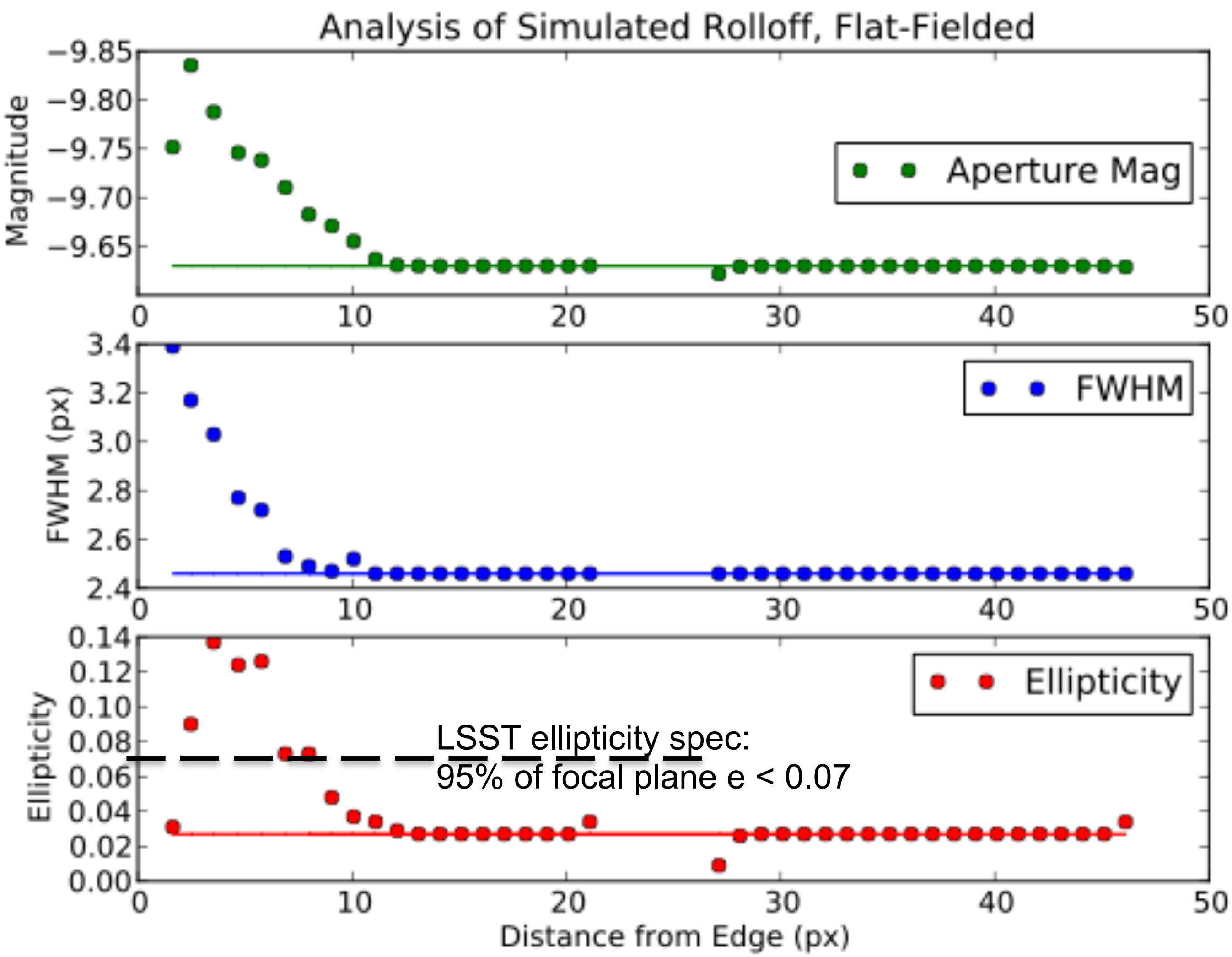

0.04 mag increases to 0.2 mag!

PSF broadening is basically unchanged

ellipticity is basically unchanged

Astrometric Errors
of order 0.8 pix = 160 milliarcsec

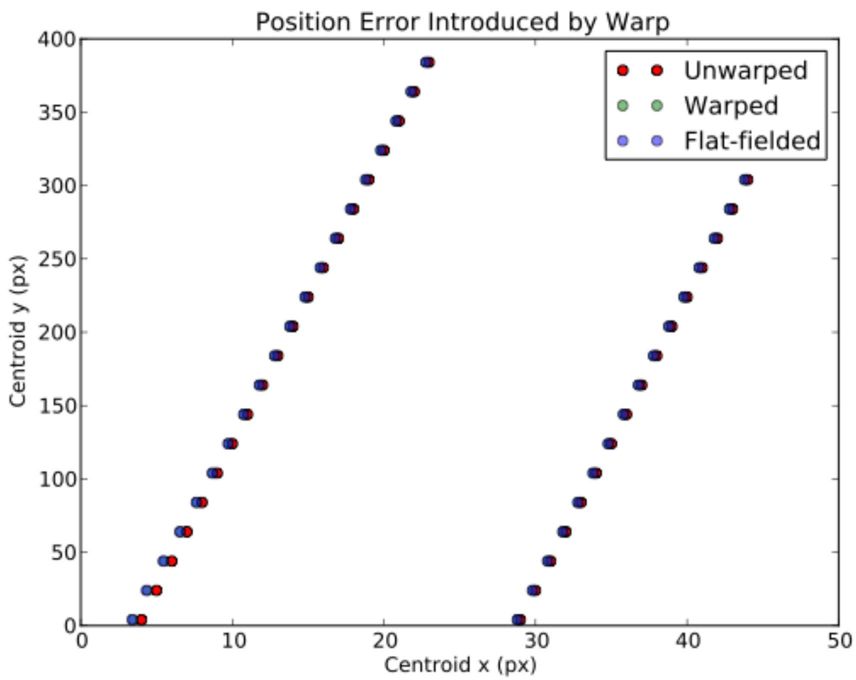

Warped vs. Unwarped Centroids

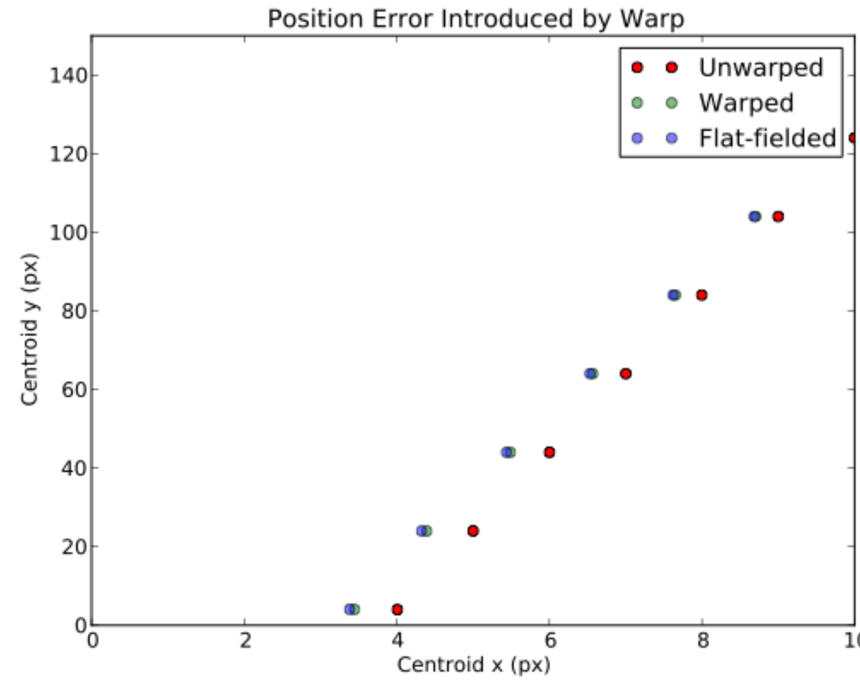

Zoomed in...

<u>Additional</u> astrometric Error Introduced by Flat-Fielding is 10%

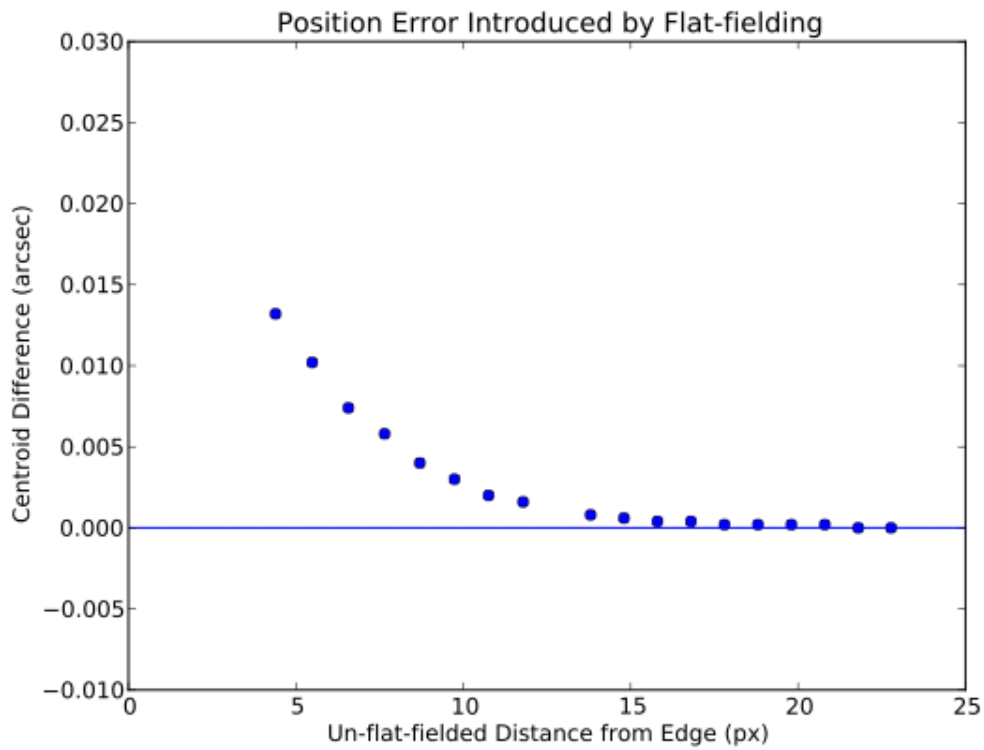

But astrometric shifts are not limited to these edge effects due to guard rings…

Impurity rings produce z-independent E fields(?)

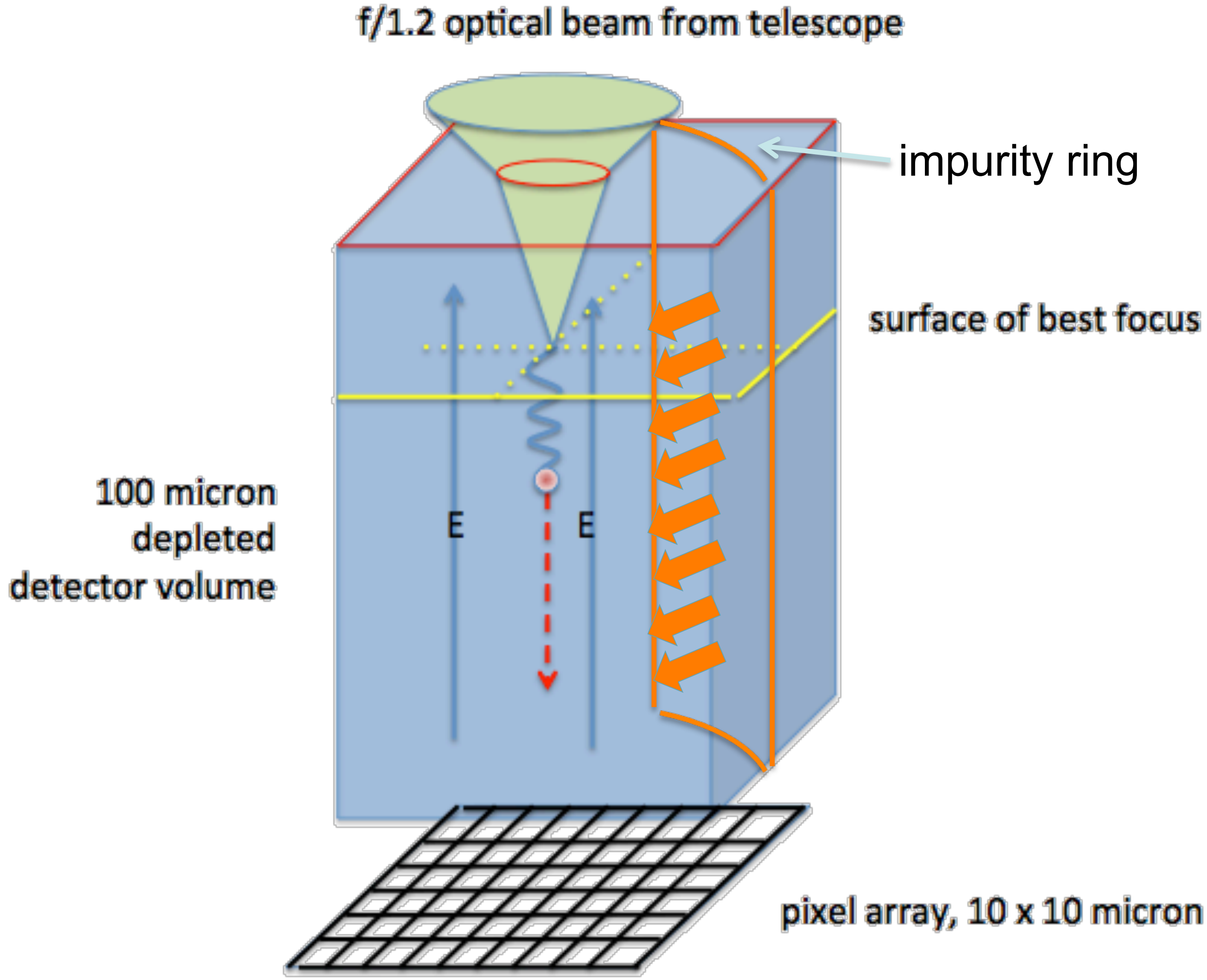

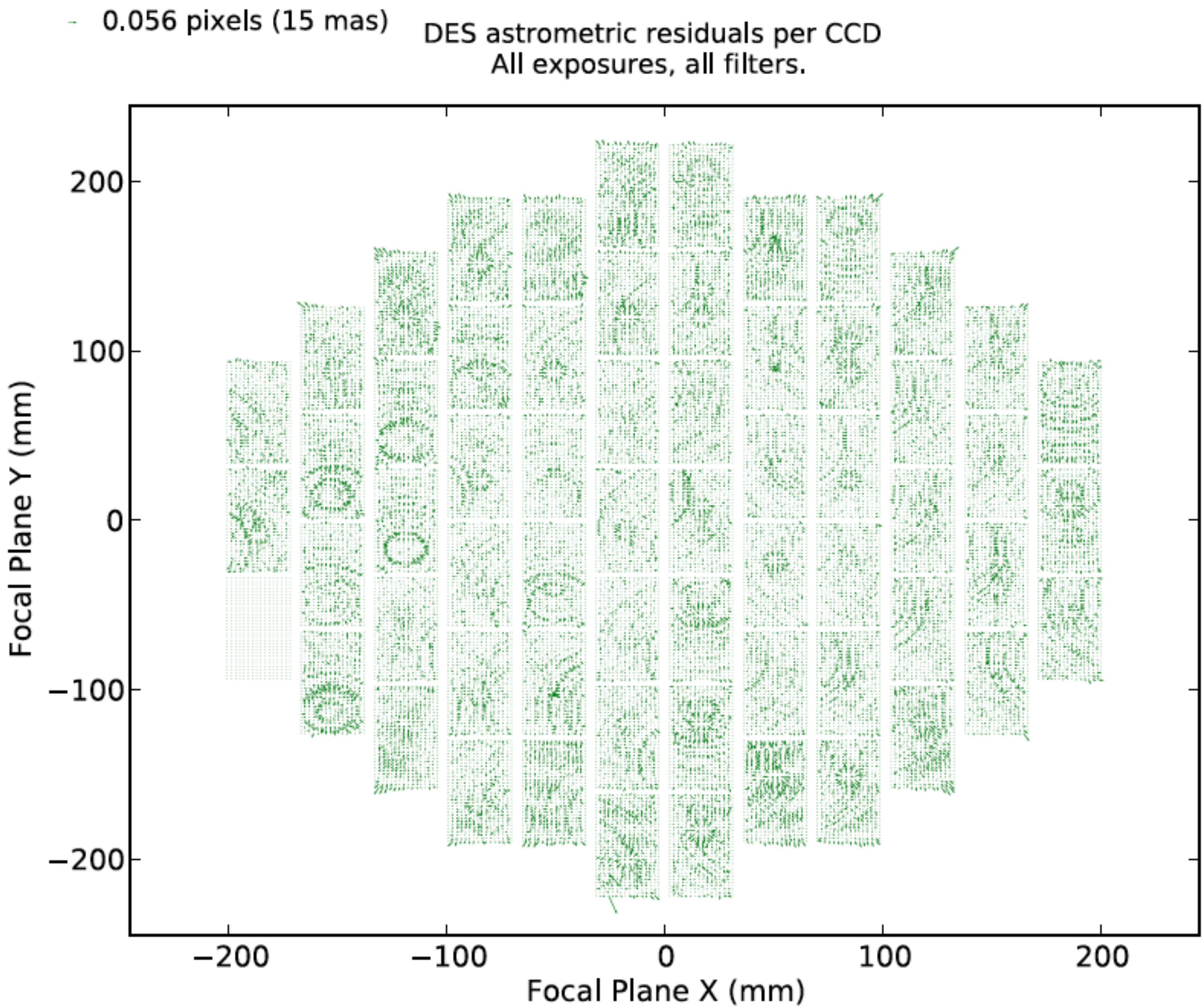
0.056 pixels (15 mas)
DES astrometric residuals per CCD
All exposures, all filters.
200
100
0
−100
−200
Focal Plane Y (mm)
−200
−100
0
100
200
Focal Plane X (mm)

Photometric errors driven by tree rings (PS1, Finkbeiner preliminary)

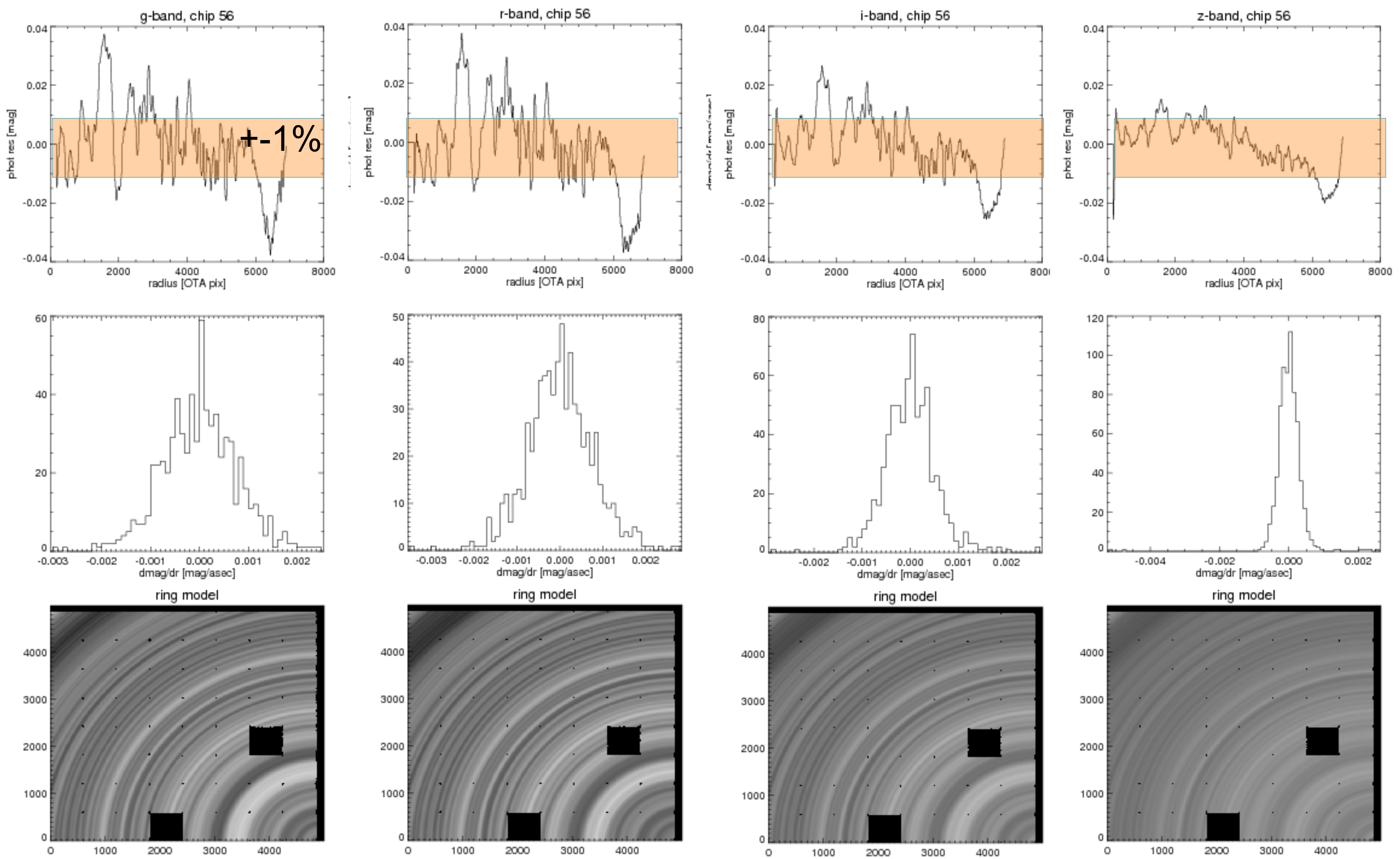

What do we learn from this, about the tree ring aspect?

- Dopant impurities produce internal lateral electric fields, presumably fairly uniform in z.
- These fields perturb the transport of photoelectrons into the pixel grid, giving rise to a distorted mapping from optical focal surface to pixels.

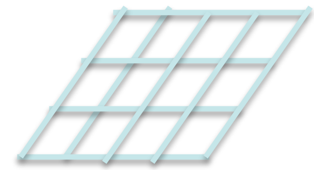

- Photoelectrons from blue photons traverse a longer distance in z, on average, than photoelectrons from red photons, so the distortion is wavelength-dependent.

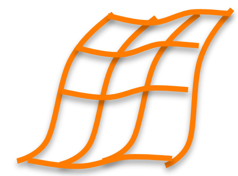

- The photometric and astrometric distortions that have been measured to correlate with the "tree ring" structure seen in flatfields are both consequences of this charge transport mapping function, and it should be something we can compensate for.
- There is also an impact on shape measurements, driven by the gradient in the 2-d "transfer function".
- We need a methodology for distinguishing these charge transport effects from actual QE variation (such as fringing).

Another (related) example-
photon transfer curve for LSST prototype devices

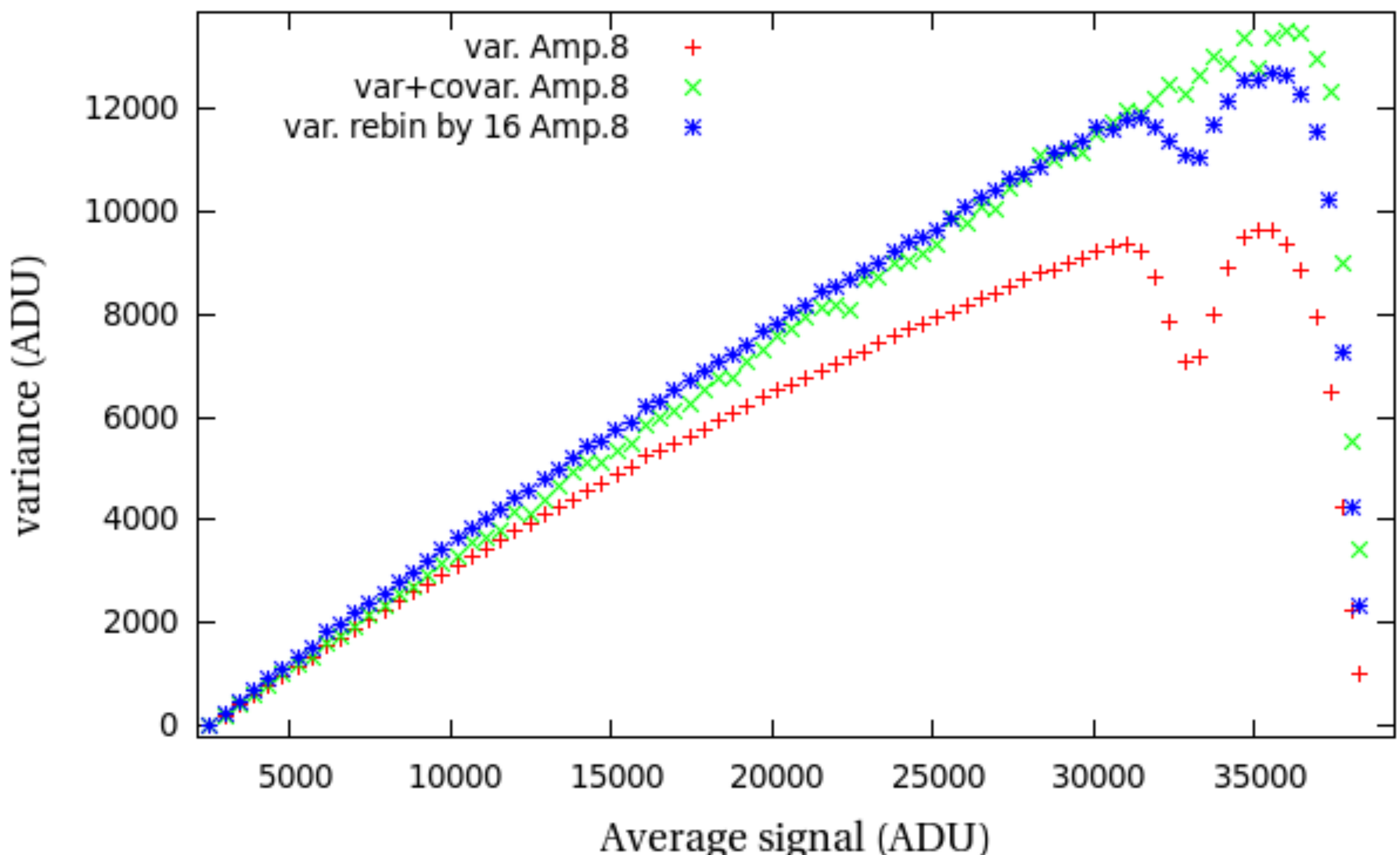

IN2P3 team, LSST sensor data

Accumulated charge in a pixel produces fields, as well…

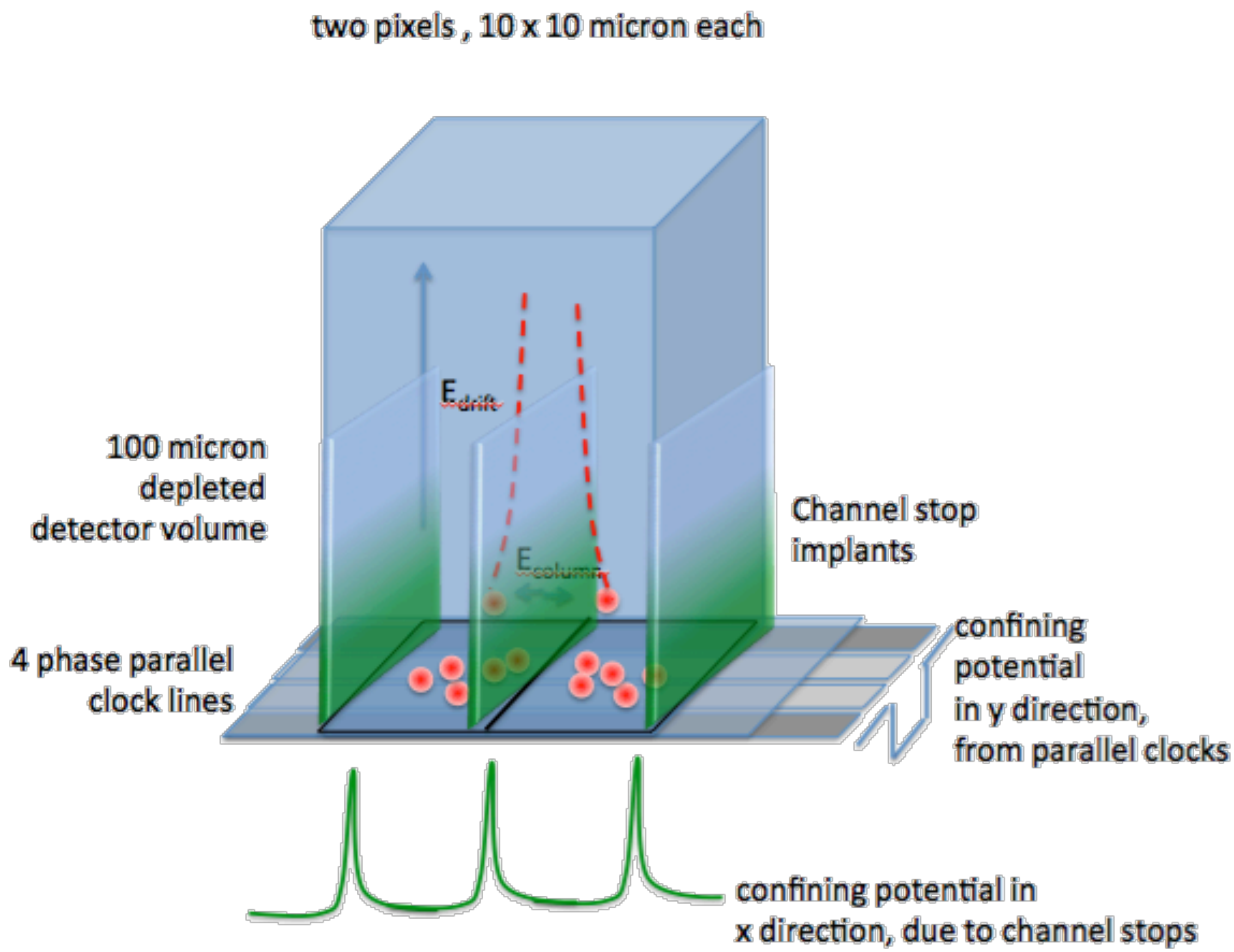

Sensor PSF effects: charge correlation

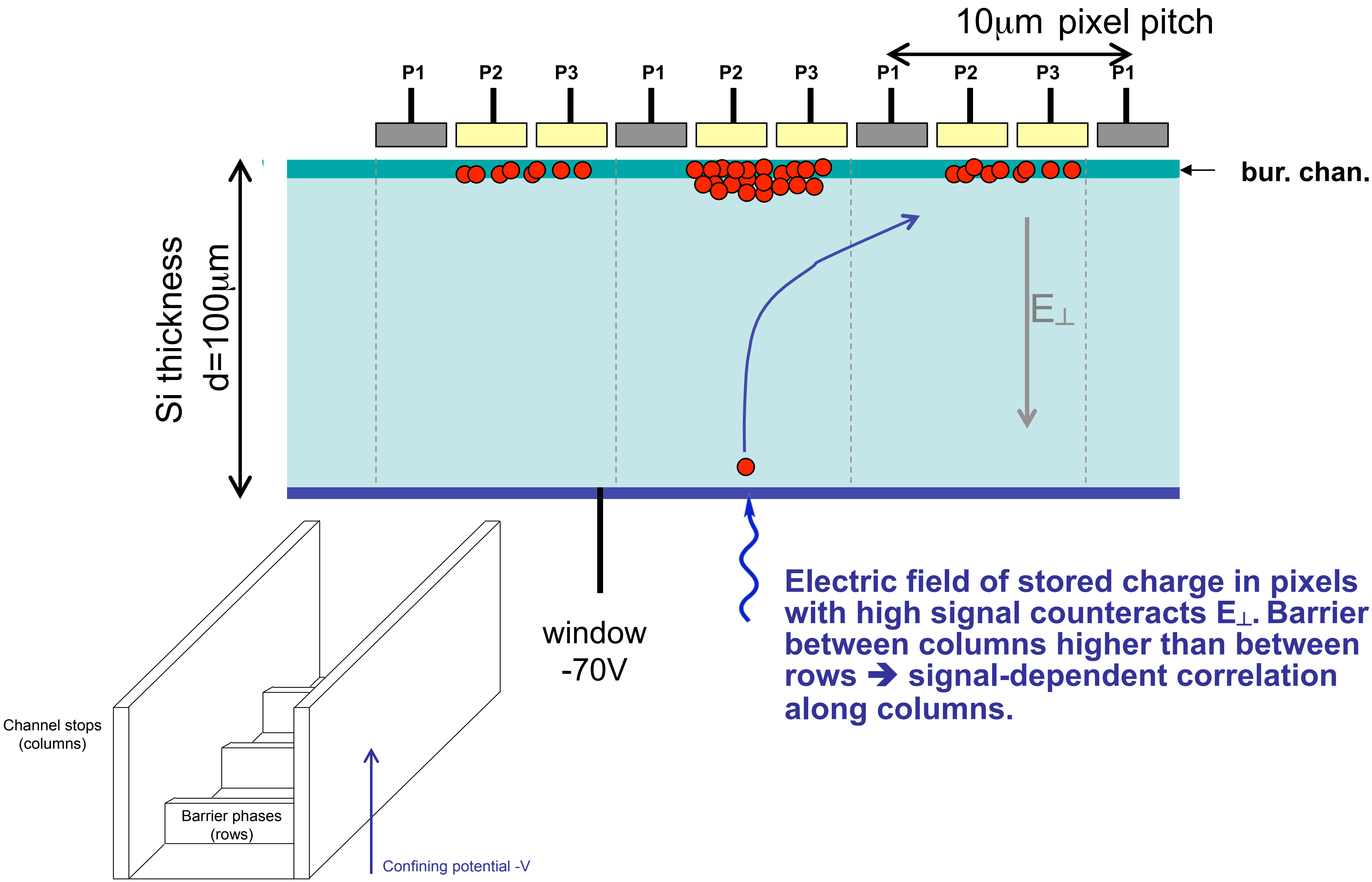

Electric field of stored charge in pixels with high signal counteracts $E_{\perp}$. Barrier between columns higher than between rows ➔ signal-dependent correlation along columns.

Intensity-dependent Lateral Fields from Space Charge Effects

from Dec 2012 report from LPHNE

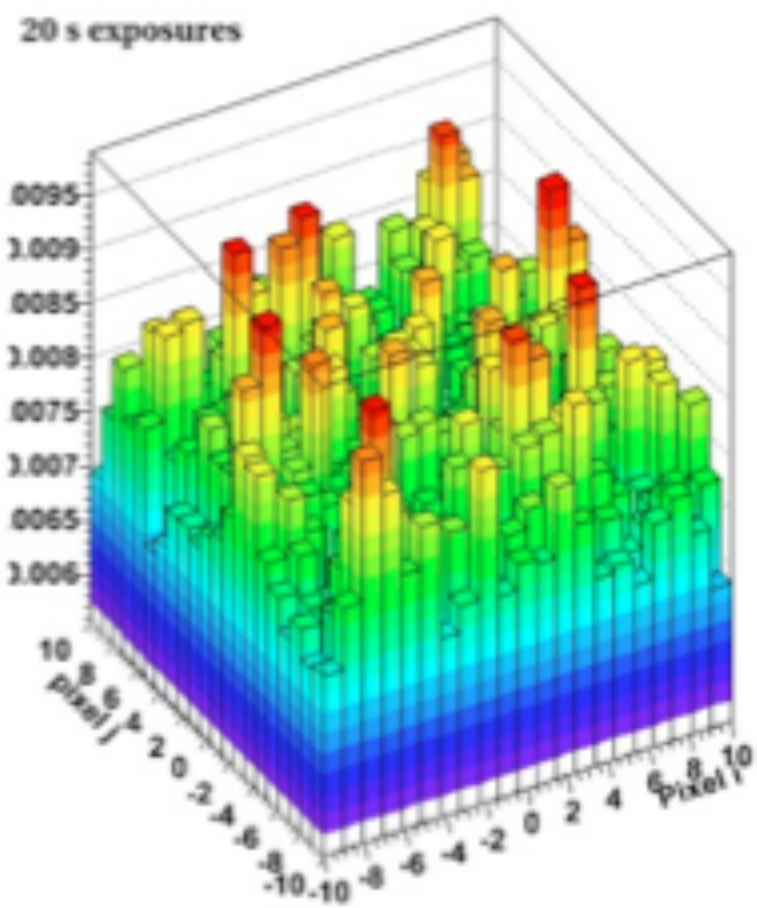

no statistical correlation at low flux

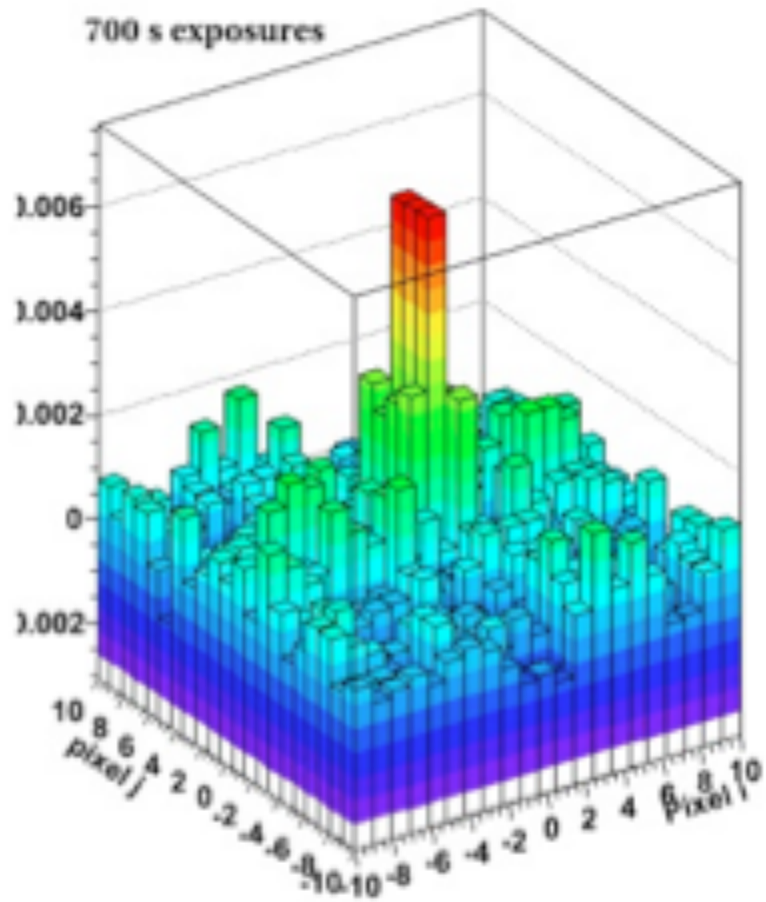

substantial correlation at high flux

2-d correlation is wavelength-independent

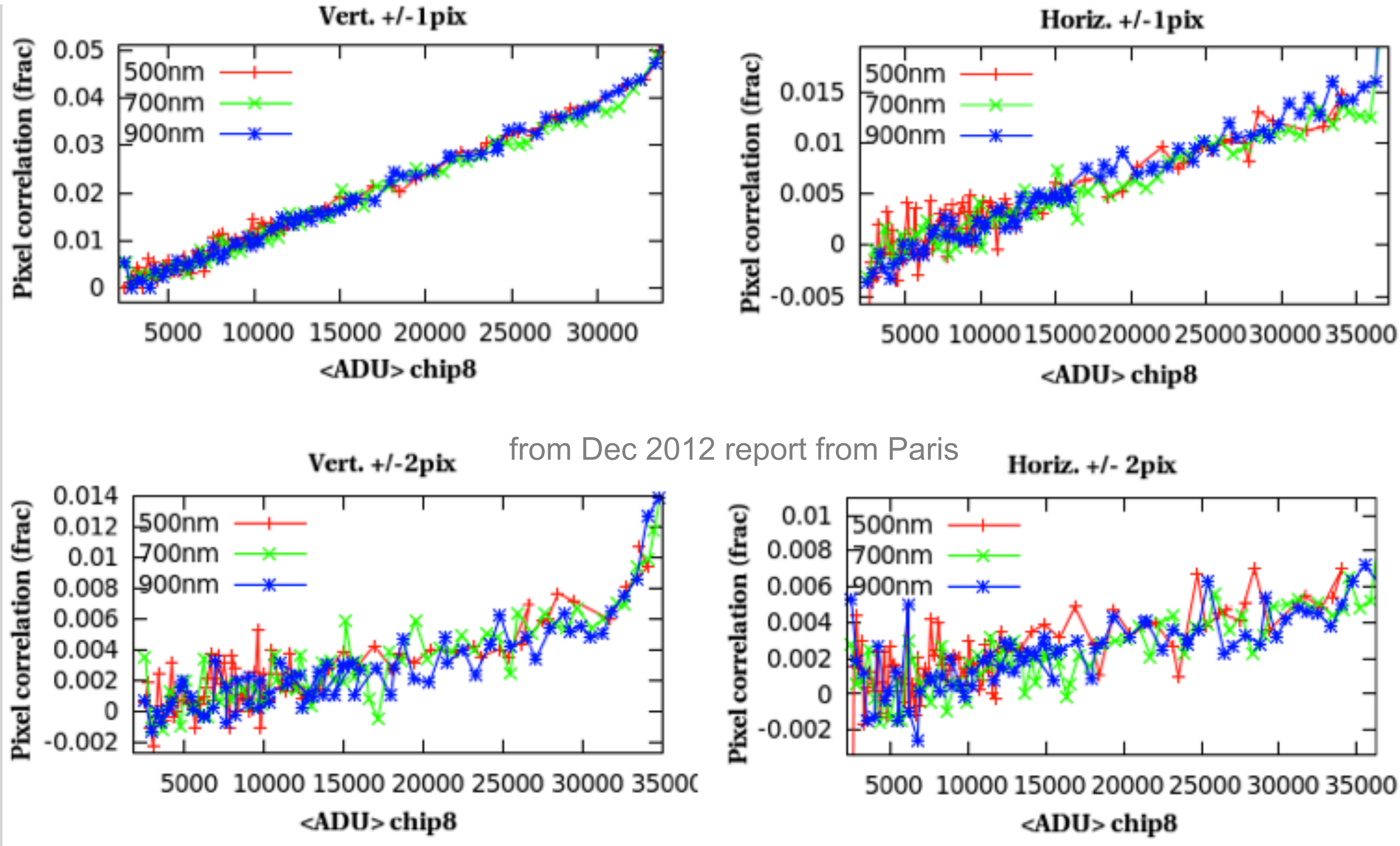

Spot profile vs. intensity: correlation-induced broadening?

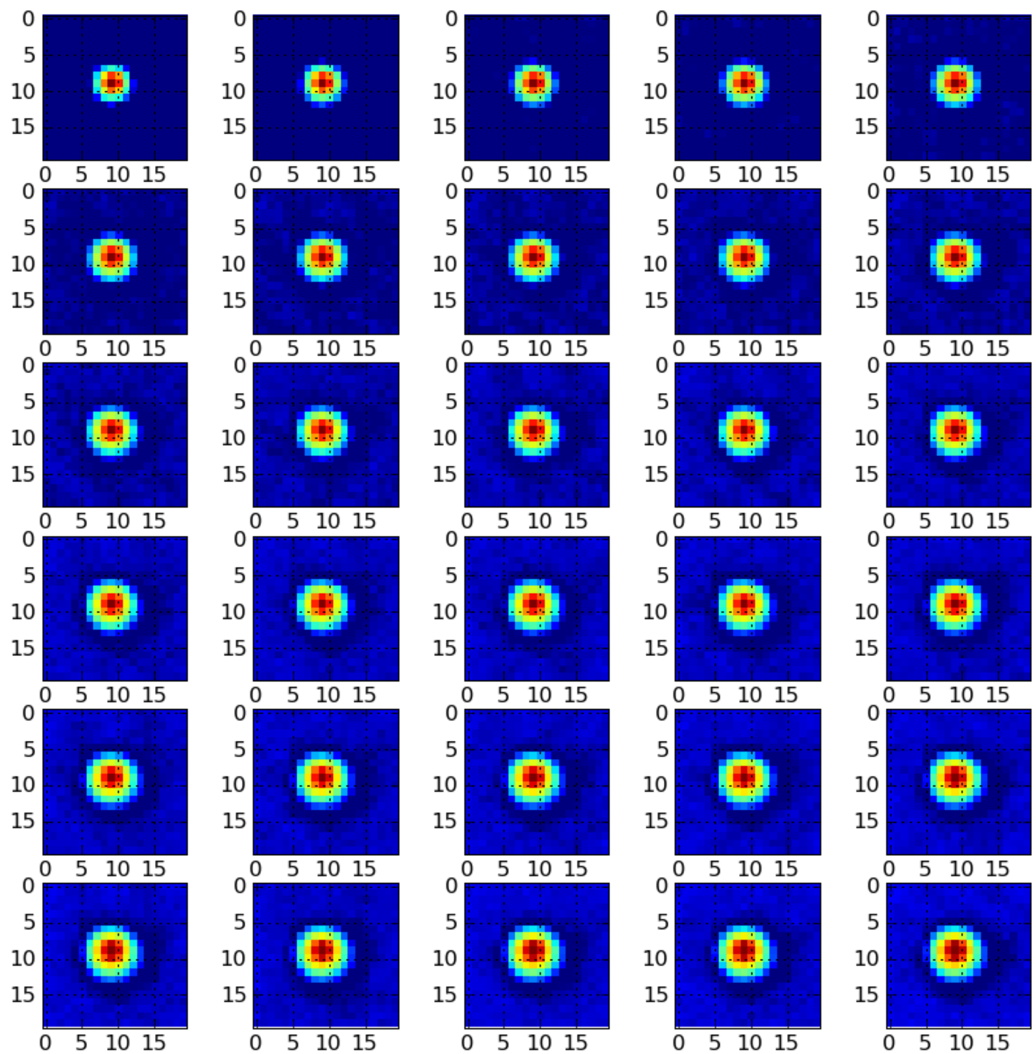

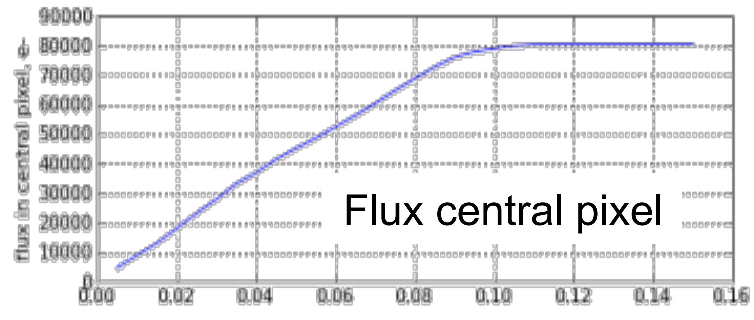

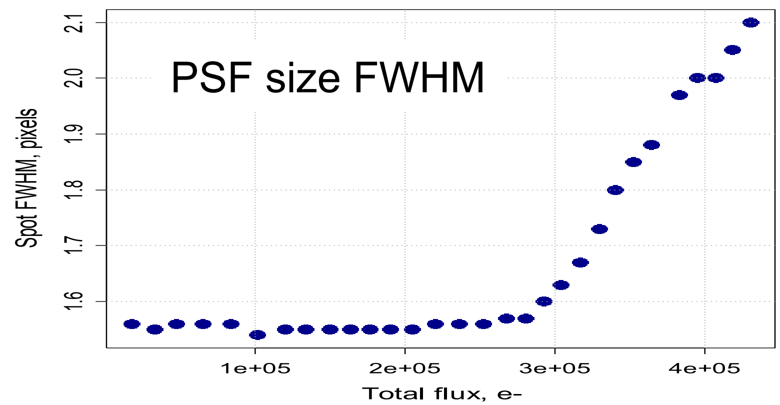

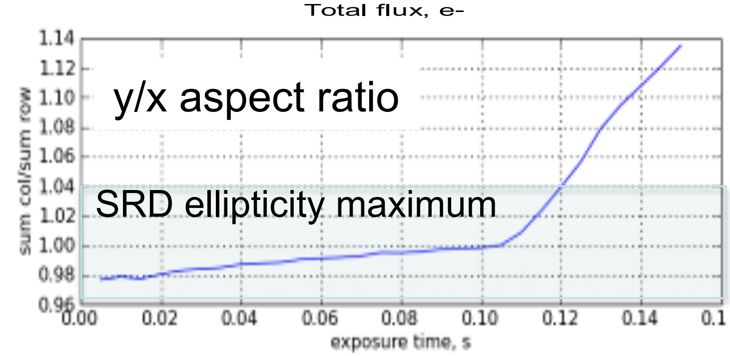

LSST DM might need to parameterize PSF by flux as well as position

Intensity-dependent PSF's

- We do see evidence for subtle distortion of PSF that depends on intensity (gradients).
- A retrospective analysis of CFHT megacam data shows this effect as well, at a lower level. This was missed by the weak lensing team that analyzed those images.
- This phenomenon is being incorporated into image simulator.
- Dark Energy Survey team has implemented a correction algorithm. Results look very promising.
- We are in constant contact with the LSST data management team on sensor and instrumental signature removal issues.

Different Sources of lateral E-fields have differing z-dependence, hence different wavelength dependence.

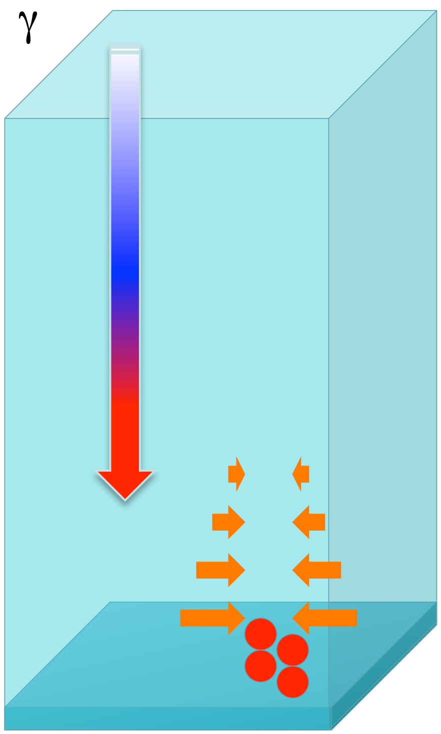

Space charge effects

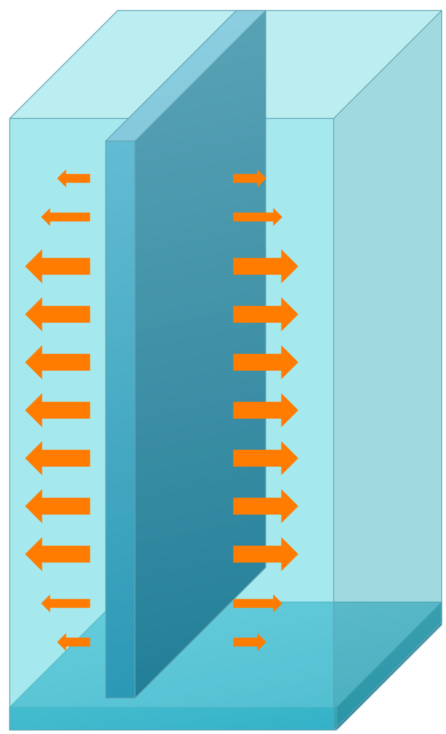

impurities

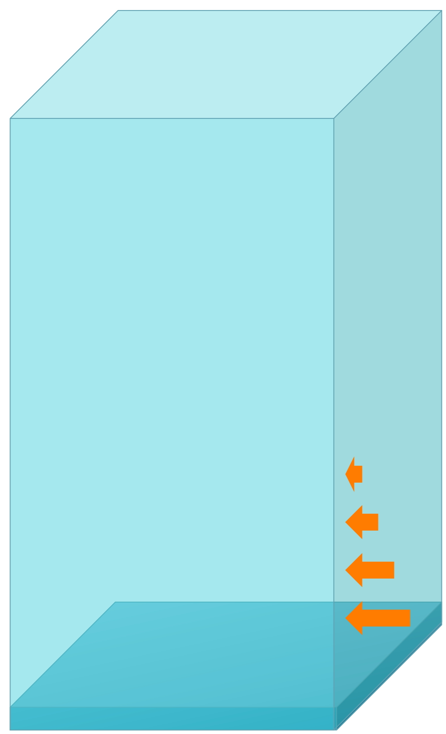

electrode effects/guard rings

Some Questions

- **How can we cleanly disentangle the contributions of genuine photon detection efficiency from various charge transport/lateral field effects?**
- **What is the optimal pixel sampling to attain best possible measurement precision? There are some characteristic length scales:**
  - Charge diffusion rms footprint
  - Pixel scale, 10-15 microns
  - Auto-correlation length in flat fields
  - Mask step-repeat scale
  - Correlation length of impurities (tree rings)
  - Coherence length of PSF shape across the focal plane, due to optics and atmosphere
  - …
- **The size of the PSF (or the size of a resolved object) compared to these scales will determine the systematic error that is introduced.**
- **Do these considerations favor using TDI (drift scanning) systems for surveys, as opposed to staring arrays with a few pixels spanning the PSF?**

How can we quantify, prioritize, calibrate and correct for these effects?

This isn't new…

In retrospect, there is a long history of charge distribution anomalies in CCDs, going to back to initial HST WFPC-1.

Historical approach to calibration and sensor sensitivity correction has been for flux measurements, and for astrometry. Naïve flat-fielding is inappropriate, and introduces systematic errors in both astrometry and photometry.

We have been working to understand the interplay between these subtle sensor properties, and shape measurements for weak lensing.

We are developing an approach that uses a combination of lab results, on-sky data, and data processing algorithms to be able to fully understand and (if needed) correct for these effects.

Quantitative determination of focal plane shape perturbations on weak lensing measurements is under way.

This phenomenology is already being incorporated into LSST simulator.

LSST team held Nov 2013 meeting on "Precision Astronomy with Deep Depletion CCDs"

Pixel-scale response perturbations *can* be circumvented

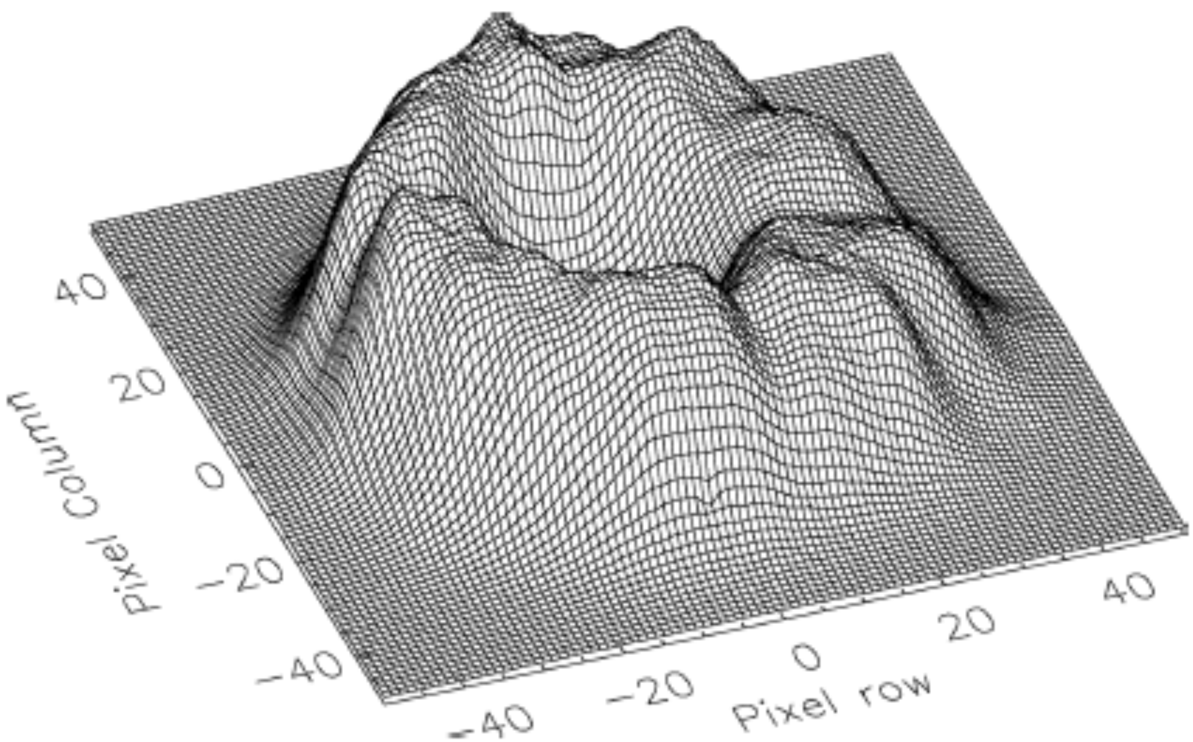

Figure 1. Surface plot of the PSF of WASP-50 in an image taken at random from the observing sequence on the night of 2011 October 24. The x and y axes are in pixels. The lowest and highest counts are 684 and 24 726 ADUs, respectively, and the z axis is on a linear scale.

WASP project uses highly defocused images to perform differential photometry of sources.

They achieve 0.2 mmag photometric precision (Tregloan-Reed & Southworth, MNRAS **431**, 996 (2013)).

200 ppm photometric precision from a ground-based telescope

0.2 mmag photometric precision (Tregloan-Reed & Southworth, MNRAS **431**, 996 (2013)).

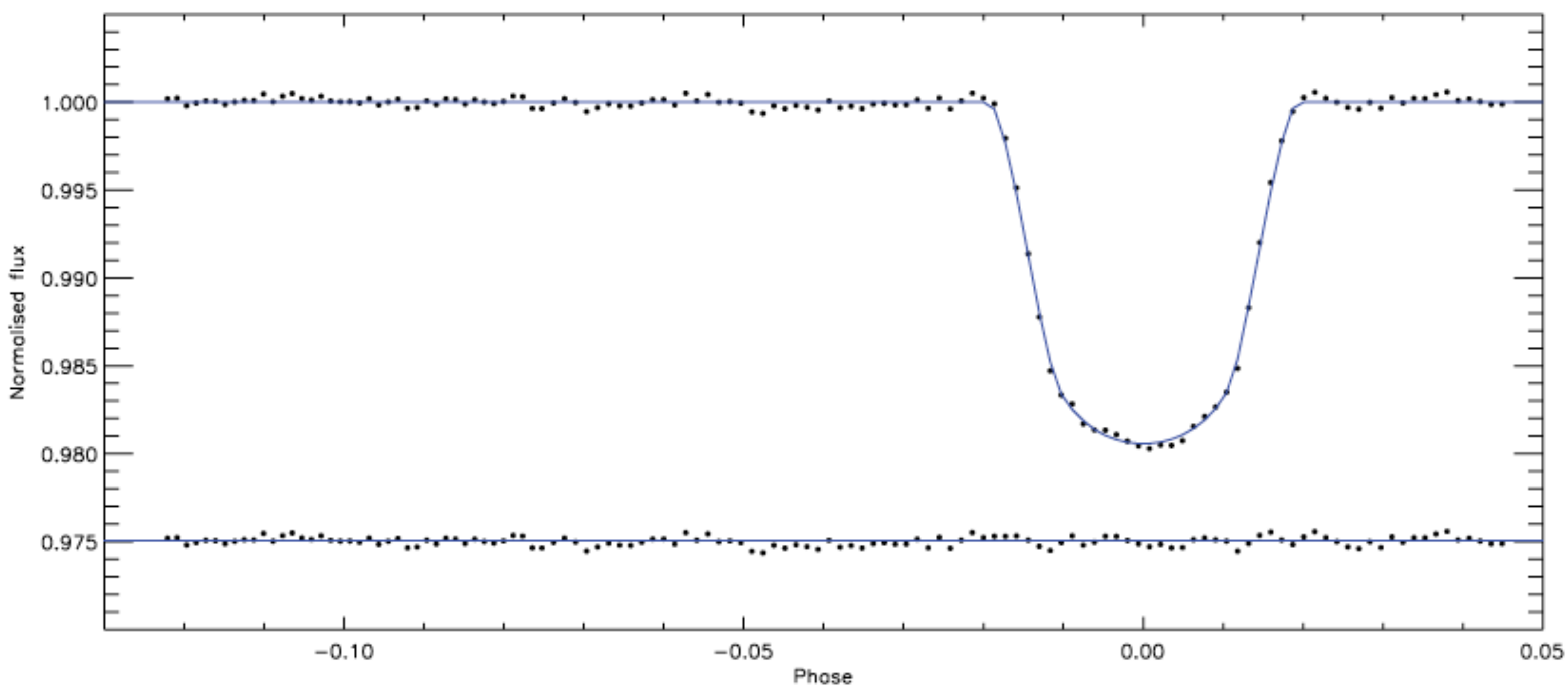

Figure 2. Transit light curve and the best-fitting model for 2011 November 20. The residuals are displayed at the base of the figure.

Summary

- Sensor delivery is the critical path item for the LSST camera.
- We have demonstrated sensors from two vendors that meet requirements.
- Phase 1 production contracts were just awarded to two vendors.
- Deep depletion CCDs exhibit features due to lateral electric fields, that we must attend to in order to achieve high precision photometry, astrometry and shape determination.
- In retrospect, these features are also apparent in previous generations of CCDs.
- We are working to develop methods to distinguish between QE variations and lateral electric field effects.
- See proceedings of Nov 2013, 2014 BNL workshops for further details.

Some pertinent resources and references

Scientific Charge Coupled Devices, Janesick
920 pages, the bible

Handbook of CCD Astronomy, Howell
220 pages, a nicely accessible starting point

2013 BNL meeting: precision astronomy with fully depleted CCDs
https://indico.bnl.gov/conferenceDisplay.py?confId=672

2014 BNL meeting: precision astronomy with fully depleted CCDs
https://indico.bnl.gov/conferenceDisplay.py?confId=878

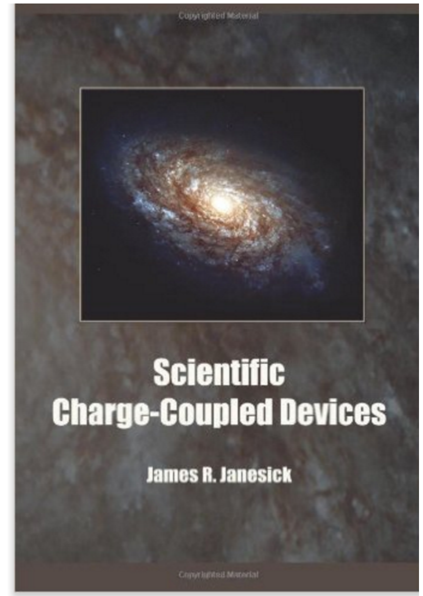

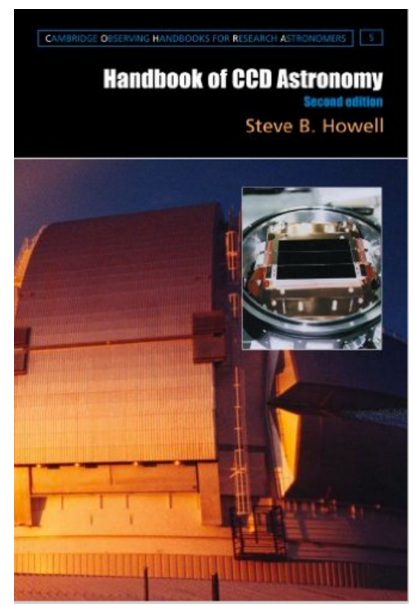

Some LSST-specific resources and references

LSST camera science raft sensor reports	ITL/STA Centerline Anti-Blooming Implant Testing	Document-14304
LSST camera science raft sensor reports	Photometric Effects at the Perimeter of the E2V CCD250	Document-14323
LSST camera science raft sensor reports	Photometric Effects at the Blooming Stop Implant of the E2V CCD250	Document-14324
LSST camera science raft sensor reports	The 'Dim Row' Observed in the E2V CCD250	Document-14325
LSST camera science raft sensor reports	Image Persistence in the E2V CCD250	Document-14326
LSST camera science raft sensor reports	E2V CCD250 PSF and pixels response sensitivity to light intensity	Document-14327
LSST camera science raft sensor reports	Amplifier to Amplifier Crosstalk in the E2V CCD250	Document-14328
LSST camera science raft sensor reports	Photometric and astrometric response of STA 1920A	Document-14329
LSST camera science raft sensor reports	SpotScan probe of edge effects in CCD250	Document-14330
LSST camera science raft sensor reports	"Tree rings" seen in deep, flat field data in CCD250	Document-14331